HDL-CR-77-081-1

FLUIDIC GUN STABILIZATION SYSTEM DEVELOPMENT PROGRAM

MARCH 1977

Prepared by

AIRESEARCH MANUFACTURING COMPANY
A DIVISION OF THE GARRETT CORPORATION
402 SOUTH 36TH STREET
PHOENIX, ARIZONA 85034

U.S. Army Materiel Development
and Readiness Comma d
HARRY DIAMOND LABORATORIES
Adelphi, Maryland 20783

The findings in this report are not
to be construed as an official Department
of the Army position unless so designated
by other authorized documents.

Citation of manufacturers' or trade
names does not constitute an official en-
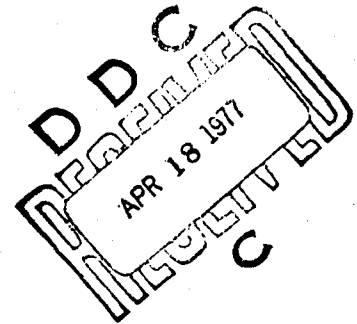dorsement or approval of the use thereof.

Destroy this report when it is no
longer needed. Do not return it to the
originator.

FLUIDIC GUN STABILIZATION SYSTEM DEVELOPMENT PROGRAM

MARCH 1977

THOMAS B. TIPPETTS
WALLIS T. FLEMING
AIRESEARCH MANUFACTURING COMPANY
A DIVISION OF THE GARRETT CORPORATION
402 SOUTH 36TH STREET
PHOENIX, ARIZONA 85034

REPORT DOCUMENTATION PAGE		READ INSTRUCTIONS BEFORE COMPLETING FORM
1. REPORT NUMBER HDL-CR-77-081-1	2. GOVT ACCESSION NO.	3. RECIPIENT'S CATALOG NUMBER
4. TITLE (and Subtitle) FLUIDIC GUN STABILIZATION SYSTEM DEVELOPMENT PROGRAM		5. TYPE OF REPORT & PERIOD COVERED Final Report for period from Mar to Nov 76.
		6. PERFORMING ORG. REPORT NUMBER 76-411592
7. AUTHOR(s) Thomas B. Tippetts Wallis T. Fleming		8. CONTRACT OR GRANT NUMBER(s) DAAG39-76-C-0081
9. PERFORMING ORGANIZATION NAME AND ADDRESS AiResearch Manufacturing Co. of Arizona A Division of The Garrett Corporation 402 South 36th St., P.O. Box 5217 Phoenix, Arizona 85034		10. PROGRAM ELEMENT, PROJECT, TASK AREA & WORK UNIT NUMBERS Prog. Ele.: 6.21.14.A DA Project: 1L162114AH73
11. CONTROLLING OFFICE NAME AND ADDRESS Department of the Army Harry Diamond Laboratories 2800 Powder Mill Road Adelphi, Maryland 20783		12. REPORT DATE March 31, 1977
		13. NUMBER OF PAGES 59
14. MONITORING AGENCY NAME & ADDRESS(if different from Controlling Office)		15. SECURITY CLASS (of this report) Unclassified
		15a. DECLASSIFICATION/DOWNGRADING SCHEDULE

16. DISTRIBUTION STATEMENT (of this Report)

Approved for public release; distribution unlimited.

17. DISTRIBUTION STATEMENT (of the abstract entered in Block 20, if different from Report)

18. SUPPLEMENTARY NOTES

DRCMS Code: 612114.H730011
HDL Project: 304734

19. KEY WORDS (Continue on reverse side if necessary and identify by block number)

Fluidic Control System
Gun Stabilization System

20. ABSTRACT (Continue on reverse side if necessary and identify by block number)

This report describes the results of a design and development program conducted by AiResearch Manufacturing Company which was intended to demonstrate the feasibility of a fluidic gun stabilization system for the elevation axis. The system utilizes an angular accelerometer with pneumatic pickoff, a pneumatic/fluidic dynamic compensation and amplification circuit, and a pneumatic/hydraulic pressure control servovalve driving the hydraulic gun → next page

DD FORM 1473 EDITION OF 1 NOV 65 IS OBSOLETE

20.   ABSTRACT (CONCLUDED)

(cont) > actuator.   The servovalve, handle valve, actuator, turret test fixture, and vehicle data used in design of the system were related to the MIC-V tank and were provided by Rock Island Arsenal.

The tasks accomplished during the program included the following:

- o   Development of system analytical models;
- o   Design and fabrication of a breadboard accelerometer-controller unit;
- o   Testing of controller components, and
- o   Demonstration of closed loop system performance for the elevation axis while installed in a full-scale turret test fixture.

TABLE OF CONTENTS

LIST OF APPENDICES

LIST OF DRAWINGS

LIST OF ILLUSTRATIONS

4

This is the final report by AiResearch Manufacturing Company of Arizona, a Division of The Garrett Corporation, under HDL Contract DAAG39-76-C-0081. The program reported herein was concerned with the development and feasibility demonstration of a fluidic gun stabilization system. The system, identified as AiResearch System 710538-1-1, is intended for installation in combat vehicles such as tanks and armored personnel carriers to assist the gunner in maintaining the gun properly aligned with the selected target while the vehicle is in motion over uneven terrain and the gun mounting is being subjected to random disturbances through the vehicle suspension system.

1. INTRODUCTION

The fluidic gun stabilization system described in this report was designed for the elevation axis only. However, the system concepts and control techniques developed for the elevation axis are also applicable to the azimuth axis, thus providing the technology for development of a completely fluidic gun control system. AiResearch has previously developed breadboard components for an azimuth axis control for the M60A1 tank under Rock Island Arsenal Contract DAAA09-74-C-2069. The elevation axis control concept employed for analytical and test evaluation consisted of an angular accelerometer and fluidic controller to attenuate external disturbances and to improve control of the elevation alignment of the gun.

2. SYSTEM ANALYSIS

The following aspects of the fluidic gun stabilization system were explored analytically:

○   A linear frequency response analysis was performed on the accelerometer-controller-gun actuation loop to gain insight into the general dynamic performance of the system.

○   A linear frequency response analysis was performed to determine the effect of controller noise on tracking accuracy.

○   An analog computer model of the system, which included system nonlinearities and gunner dynamic performance, was studied to obtain information on overall system performance.

Figure 1 presents a block diagram of the tank gun elevation control system which utilizes two hydraulic valves. Inputs from the gunner enter the system via the control handle which is connected directly to the gunner's control valve. The tracking velocity of the gun is controlled by displacement of the handle. The second valve is a pneumatic/hydraulic pressure control servovalve, driven by the dynamically compensated output of the fluidic accelerometer. Also included is a handle rate pickoff which functions to suppress the accelerometer feedback signal when the gunner desires to change the commanded tracking rate. The dynamic transfer function representing the gunner was obtained by averaging the time constants contained in the first two functions on Page 350 of Reference 1. Because of the

----

1. Bioastronautics Data Book, NASA Report SP-3006

FIGURE 1

HDL/RIA GUN STABILIZATION SYSTEM
MIC-V TANK WITH 20MM GUN
MOOG SERVOVALVE MODEL 15-010
4-16-76 (REV. A 4-23-76)

PARAMETERS

SYMBOLS	UNITS	DESCRIPTION
A_H	IN²	VALVE SPOOL COMMAND LAND AREA
A_L	IN²	VALVE SPOOL FEEDBACK LAND AREA
f_s	LB SEC/IN	SPOOL FRICTION
X_{MM}	IN	MAXIMUM SPOOL STROKE (SERVOVALVE)
Q_{MM}	IN³/SEC	MAXIMUM VALVE FLOW RATE (SERVOVALVE)
K_D	IN³/SEC	SERVOVALVE DROOP CONSTANT
P_s	PSI	HYDRAULIC SUPPLY PRESSURE
C	IN³/LB	HYDRAULIC CAPACITANCE
A_p	IN²	ACTUATOR PISTON AREA
I	LB-FT-SEC²	GUN MOMENT OF INERTIA
f_g	IN LB SEC/IN	FRICTION REFERRED TO GUN ANGLE
f_a	LB SEC/IN	FRICTION REFERRED TO ACTUATOR DISPLACEMENT
A_r	IN	ACTUATOR MOMENT ARM
GD	DIMENSIONLESS	GUN BENDING DYNAMICS
HD	DIMENSIONLESS	HULL SUSPENSION DYNAMICS
AD	DIMENSIONLESS	ACCELEROMETER DYNAMICS

SYMBOLS	UNITS	DESCRIPTION
K_L	SEC	ACCELEROMETER LOOP GAIN
K_1	DIMENSIONLESS	GUNNER GAIN INTO HANDLE VALVE
K_2	DIMENSIONLESS	GUNNER GAIN INTO HANDLE RATE PICKOFF
τ_d	SEC	DIFFERENTIATOR TIME CONSTANT
τ_1	SEC	LEAD TIME CONSTANT
τ_2	SEC	LAG TIME CONSTANT
τ_c	SEC	SERVOVALVE INPUT TIME CONSTANT
K_v	LB SEC/LB²	SERVOVALVE GAIN
Q_{HMM}	IN³/SEC	HANDLE VALVE MAXIMUM FLOW
X_{HMM}	IN	HANDLE VALVE MAXIMUM STROKE
K_{LK}	IN³/LB SEC	LEAKAGE CONSTANT

VARIABLES

SYMBOLS	UNITS	DESCRIPTION
θ_T	RAD	TARGET ELEVATION ANGLE
θ_G	RAD	GUN ELEVATION ANGLE
θ_B	RAD	TERRAIN ELEVATION ANGLE
$\dot{\theta}_H$	RAD/SEC	HULL ELEVATION RATE
$\ddot{\theta}_H$	RAD/SEC²	INDICATED GUN ACCELERATION
$\dot{\theta}_c$	RAD/SEC	COMMAND GUN ELEVATION RATE
P_R	PSID	COMMANDED ACTUATOR PRESSURE
P_L	PSID	ACTUATOR PRESSURE
F	LB	SPOOL FORCE
x	IN	SPOOL DISPLACEMENT
Q	IN³/SEC	HYDRAULIC FLOW RATE
$\dot{y}$	IN/SEC	ACTUATOR VELOCITY
Q_H	IN³/SEC	HANDLE VALVE FLOW
X_H	IN	HANDLE VALVE STROKE
s	1/SEC	LAPLACE VARIABLE

Block diagram labels: TERRAIN ELEVATION, HULL MOTION, GUN ELEVATION, HANDLE VALVE, HANDLE RATE PICKOFF, DYNAMIC COMPENSATION, SERVOVALVE FLUIDIC INPUT, SERVOVALVE, ACTUATOR, ACCELEROMETER, GUNNER, TARGET ELEVATION

presumed ability of the gunner to adapt himself to a particular control task, the gain in the gunner transfer function was adjusted to a value that gave optimum response and stability.

To concentrate the analysis on those parameters which have a significant effect on system performance, the system block diagram was reduced to that shown on Figure 2. The procedure and justification for this reduction is outlined in Appendix A.

2.1 Linear System Analysis

Dynamic performance of the gun stabilization system was explored by means of a frequency response analysis of the accelerometer loop shown in Figure 2. The effects on disturbance suppression of variations in the lead time constant, τ_1, the lag time constant, τ_2, and the servovalve time constant, τ_3, were evaluated.

Disturbance suppression is given by the following function (for $\ddot{\theta}_C = 0$):

$$\frac{\theta_G}{\theta_H} = \frac{1}{(1 + \tau_G S)(1 + K_L \, GH)}$$

where

$$GH = \frac{(1 + \tau_1 S)(S)}{(1 + \tau_G S)(1 + \tau_2 S)(1 + \tau_3 S)(\frac{S^2}{\omega_n^2} + 2\zeta \frac{S}{\omega_n} + 1)}$$

The amplitude of this function is plotted versus frequency in Figures 3, 4, and 5 for various values of τ_1, τ_2, and τ_3, respectively. The loop gain, K_L, was set at a value which gave a stability gain margin of 10 db for each case. The effectiveness of the stabilization system in suppressing disturbances is measured by the amount that the curves fall below zero decibels.

Figure 3 illustrates the effect of the lead time constant on disturbance suppression. Comparison of Curve 1 with Curve 4 on Figure 3 demonstrates that omission of the lead factor results in significant degradation. In other calculations, no significant improvement was noted when other parameters were varied as long as the value of τ_1 remained equal to zero. Inclusion of a lead time constant of $\tau_1 = 0.05$ second resulted in the optimum suppression which is depicted in Curve 4 on Figure 3.

9

TERRAIN
ELEVATION
θ_B

HULL
SUSPENSION
DYNAMICS

$$\frac{1}{\frac{s^2}{\omega_H^2} + \frac{2\zeta_H}{\omega_H}s + 1}$$

θ_H·

s

θ_H

K_1

GUN
ELEVATION

$$\frac{K_2 s}{1 + \tau_3 s}$$

$$\frac{1 + \tau_1 s}{1 + \tau_2 s}$$

K_L

$$\frac{1}{1 + \tau_3 s}$$

$$\frac{s}{1 + \tau_G s}$$

$\ddot{\theta}_G$

$$\frac{1}{s}$$

$\dot{\theta}_G'$

$$\frac{1}{s}$$

θ_G

ACCELEROMETER

$$\frac{1}{\frac{s^2}{\omega_n^2} + \frac{2\zeta}{\omega_n}s + 1}$$

$\dot{\theta}_G$

GUNNER

$$e^{-0.2s} \frac{1 + \frac{s}{0.8}}{1 + \frac{s}{0.13}}$$

θ_T TARGET
ELEVATION

$$\tau_G = \frac{I}{(\text{A SIN}\beta)^2 \left[K_Q A_P^2 + b\right]}$$
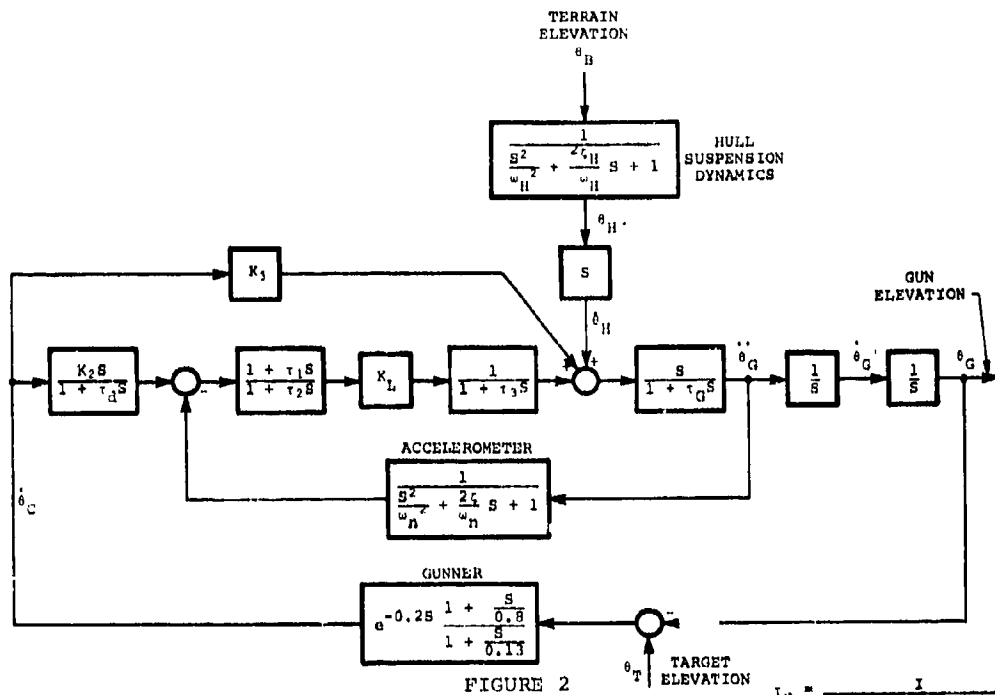
FIGURE 2

LINEARIZED BLOCK DIAGRAM FOR
HARRY DIAMOND LABORATORIES/ROCK ISLAND ARSENAL,
GUN STABILIZATION SYSTEM
MIC-V TANK WITH 20MM GUN

ω_n = 49 RADIANS PER SECOND
ζ = 1
τ_G = 0.7 SECOND (ACTUATOR
  AREA = 0.89 SQUARE INCH)
τ = 2.0 SECONDS
τ_3 = 0.01 SECOND

① = 0, K_L = 26.6
② = 0.2 SECOND, K_L = 19.9
③ = 0.1 SECOND, K_L = 35
④ = 0.05 SECOND, K_L = 56

FREQUENCY, HZ
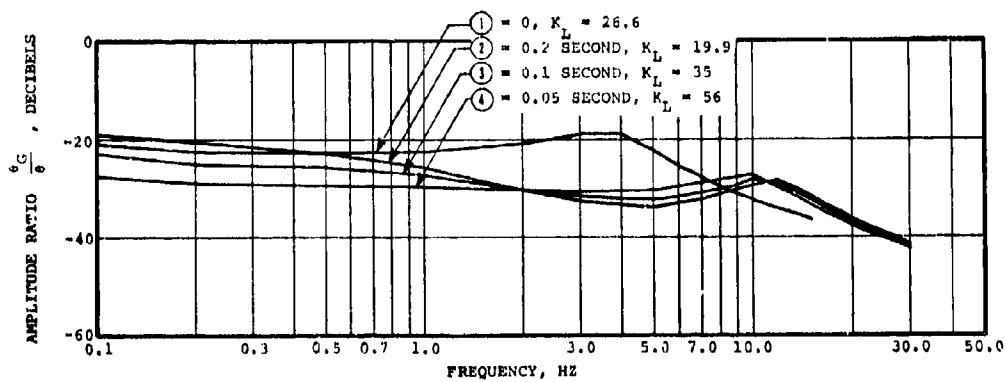
FIGURE 3

EFFECT OF LEAD TIME CONSTANT ON
DISTURBANCE SUPPRESSION OF
GUN STABILIZATION SYSTEM

10
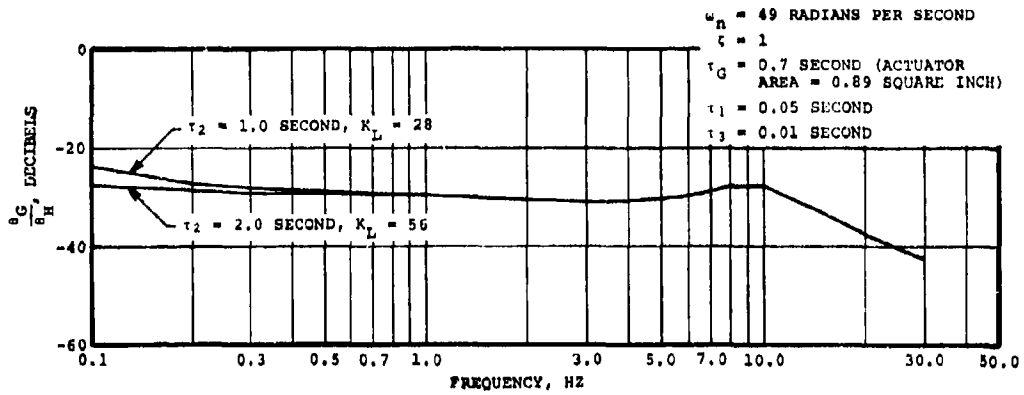
FIGURE 4

EFFECT OF LAG TIME CONSTANT ON
DISTURBANCE SUPPRESSION OF
GUN STABILIZATION SYSTEM
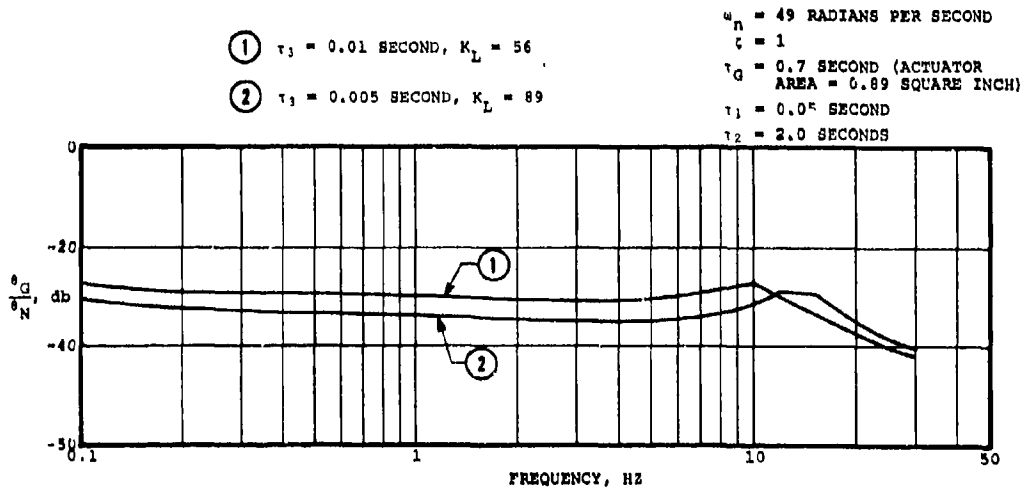
FIGURE 5

EFFECT OF SERVOVALVE TIME CONSTANT ON
DISTURBANCE SUPPRESSION OF
GUN STABILIZATION SYSTEM

11

Figure 4 illustrates the minimal effect of variations in the lag time constant, τ_2. Reduction of τ_2 from 2.0 seconds to 1.0 second results in degradation only at a very low frequency.

Figure 5 illustrates the effect of the time constant representing the response of the fluidic/hydraulic servovalve interface. These curves indicate that the time constant of the servovalve should be decreased to a value as small as practical within the power limitations of the fluidic circuit.

2.2 Controller Noise Analysis

An indication of the behavior of the gun stabilization system in response to noise generated within the controller was obtained by studying the block diagram in Figure 6.
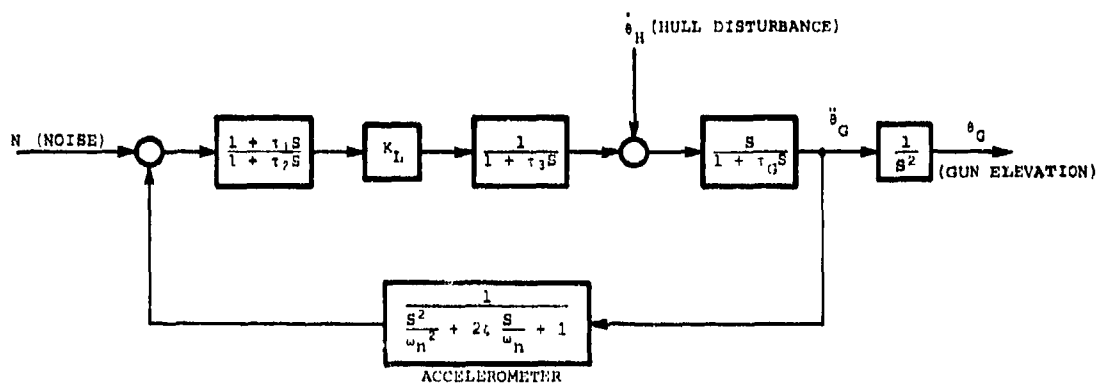
FIGURE 6

BLOCK DIAGRAM FOR NOISE ANALYSIS

The transfer function of gun elevation for noise input is given by the following:

$$\frac{\theta_G}{N} = \frac{1}{S^2} \frac{G}{1 + GH}$$

where

$$G = \frac{(1 + \tau_1 S) \, K_L \, S}{(1 + \tau_2 S)(1 + \tau_3 S)(1 + \tau_G S)}$$

$$H = \frac{1}{\dfrac{S^2}{\omega_n^2} + 2\zeta \dfrac{S}{\omega_n} + 1}$$

from which the amplitude of gun motion in response to controller noise is obtained as

$$\left| \frac{\theta_G}{N} \right| = \left| \frac{1}{S^2} \frac{G}{1 + GH} \right| \quad S \to j\omega.$$

Controller noise amplitude was obtained by observing oscilloscope traces of controller output with the volume cans removed to eliminate the filtering effect of the lag-lead compensator. Noise amplitude distribution with respect to frequency appeared to be approximately Gaussian, with a center frequency of 3.3 Hz, a standard deviation of 1.1 Hz, and a maximum peak-to-peak amplitude of 0.0046 radian per second^2 (0.04 psi assuming

loop gain $K_L = 55$ and $\dfrac{\Delta P_F}{\ddot{\theta}_G} = 0.1572$ psid per radian per second^2).

Thus

$$|N| = 0.0046 \, e^{-1/2 \left(\frac{f - 3.3}{1.1} \right)^2}$$

so that the amplitude of gun motion in response to controller noise is:

$$|\theta_G| = \left| \frac{\theta_G}{N} \right| \, |N|$$

$$|\theta_G| = \left| \frac{\theta_G}{N} \right| \, 0.0046 \, e^{-1/2 \left(\frac{f - 3.3}{1.1} \right)^2}.$$

It is evident from the plot of amplitude as a function of frequency in Figure 7 that, although the system accommodates controller noise very well at the center frequency of 3.3 Hz, the system is sensitive to noise at low frequencies. The effect of this characteristic is to cause a slow drift in response to variations in supply pressure or other disturbances to the system.

13

τ_1 = 0.05 SECOND
τ_2 = 2.0 SECOND
τ_G = 0.7 SECOND
τ_3 = 0.01 SECOND
K_L = 55
ω_n = 49 RADIANS PER SECOND
ζ = 1.0
f_O = 3.3 HZ
σ = 1.1 HZ
$|N|_{MAX}$ = 0.0046 RADIAN PER SECOND^2
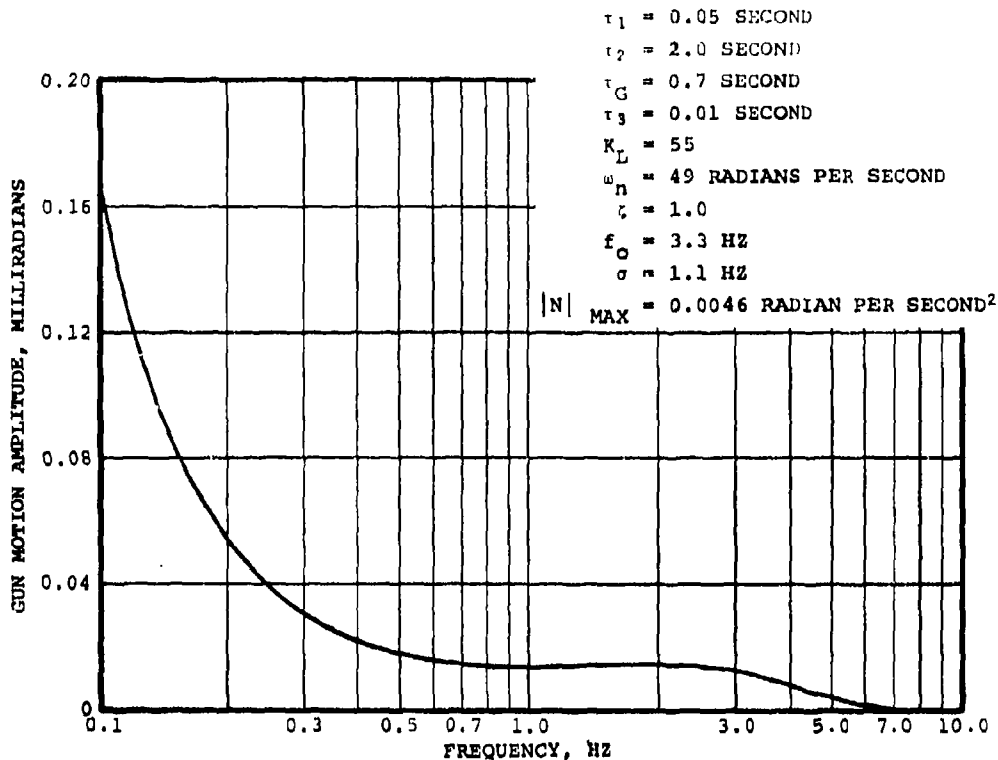
FIGURE 7

EXPECTED GUN MOTION AMPLITUDE
RESULTING FROM CONTROLLER NOISE

2.3 Analog Computer Simulation

The following paragraphs describe the analog computer
simulation of the system.

2.3.1 Method of System Analysis – To evaluate the effects of
accelerometer non-linearities and to determine optimum values
of controller parameters, the gun elevation control system was
modeled on an analog computer. In an accelerometer-stabilized
system, the gunner is considered to be the primary controller,
performing the target acquisition and tracking function while
the accelerometer loop provides assistance in steadying the
gun as the tank hull is being subjected to high frequency
motions over the terrain. Since the gunner is an essential
part of the control system, his dynamic performance was

14

included in the analog model. The analog computer circuit used
to implement the reduced system block diagram is presented in
Figure 8.

The circuit was programmed on the EAI 680 analog computer.
The output of the computer was available as a time trace on a
multi-channel strip chart recorder. The computer output could
also be processed to yield frequency response information by
use of a Bafco phase/gain analyzer.

The effects of the following parameters were evaluated:

ω_n = Accelerometer bandwidth

ζ = Accelerometer damping ratio

D = Accelerometer threshold

A_p = Hydraulic actuator piston area

Values of other parameters were fixed as follows:

τ_1 = 0.1 second

τ_2 = 2.0 seconds

τ_3 = 0.01 second

τ_d = 0.05 second

ω_H = 25 radians per second (4.0 Hz)

ζ_H = 0.1

2.3.2 <u>Results of System Analysis</u> - Figures 9 through 13 show
the effects of variations in several system parameters on the
ability of the gun stabilization system to reduce gun motion
when the tank hull is traveling at various speeds over a
sinusoidal terrain. These curves were obtained by applying a
signal representing a sinusoidally varying terrain with an
amplitude of 1.6 degrees (0.0279 radian) to the analog model
at the θ_B input and observing the signal representing gun

angle, θ_G. The ratios (in decibels) of the amplitudes of gun
angle to terrain angle are plotted as a function of terrain
frequency. The effectiveness of the stabilization system in
suppressing disturbances is measured by the amount that the

15

FIGURE 8

ANALOG CIRCUIT-GUN
STABILIZATION SYSTEM

curves fall below zero decibels. A value of minus 28.9 db represents a gun motion of 0.001 radian in response to a hull motion of 0.030 radian. In each case, the loop gain, K_L, was set at a value that gave reasonably stable performance.

The three curves that appear in each of Figures 9, 10, 12, and 13 demonstrate the effect of accelerometer threshold or deadband on the ability of the system to suppress gun motion. As expected, an increased threshold level decreases the effectiveness of the system. A threshold value of 0.003 radian per second^2 is attainable with a 40 radian per second accelerometer of six-inch diameter.

Figure 9 represents the suppression obtainable with the existing actuator with a piston area of 2.0 square inches. The peak occurring at 0.8 Hz represents the boundary between the low frequency range where the gunner provides suppression and the high frequency range where the gun stabilization system provides suppression. The peak occurring at 4 Hz is caused by the underdamped hull suspension system going into resonance, resulting in oscillation of the tank hull at a greater amplitude than terrain oscillation. Performance exhibited by this case is poor since the suppression obtainable with a threshold of 0.012 radian per second is only minus 15 db at a frequency of 0.8 Hz. It is noted that doubling of the accelerometer bandwidth as shown in Figure 10 is of no value in improving suppression of disturbances.

Figure 11 represents the disturbance suppression obtainable when the actuator piston area, A_p, is decreased to 0.89 square inch. The improved suppression is a result of decreased hull coupling as reflected in the increased value of τ_G.

Figure 12 shows the effect of varying the accelerometer damping ratio, ζ. These curves indicate that a higher loop gain, K_L, and therefore better suppression, is attainable when the damping ratio is fairly high.

Figure 13 also indicates that increased accelerometer bandwidth is of no value when the actuator piston area is decreased.

Figure 14, which is included for comparison purposes, indicates the disturbance suppression obtained when the accelerometer gain, K_L, is set at zero. This represents the suppression provided by the gunner alone when disturbances are attenuated only by the dynamics of the hull suspension and hydraulic actuation system.

17

ω_n (ACCELEROMETER BANDWIDTH) = 40 RADIANS PER SECOND
ζ (ACCELEROMETER DAMPING RATIO) = 1.0
D (ACCELEROMETER THRESHOLD) = 0.012, 0.025, 0.050 RADIANS PER SECOND^2
A_P (ACTUATOR AREA) = 2 SQUARE INCHES
K_L (ACCELEROMETER LOOP GAIN) = 21
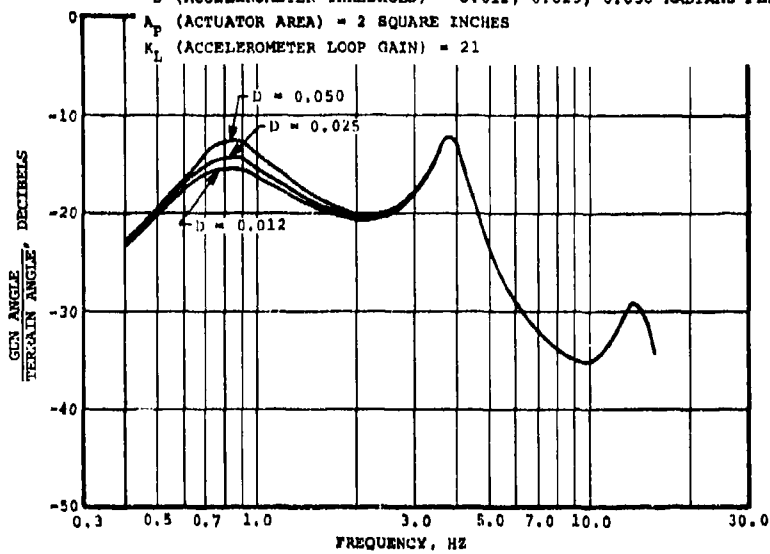
FIGURE 9

DISTURBANCE SUPPRESSION WITH
GUN STABILIZATION SYSTEM

ω_n (ACCELEROMETER BANDWIDTH) = 80 RADIANS PER SECOND
ζ (ACCELEROMETER DAMPING RATIO) = 1.0
D (ACCELEROMETER THRESHOLD) = 0.012, 0.025, 0.050 RADIANS PER SECOND^2
A_P (ACTUATOR AREA) = 2.0 SQUARE INCH
K_L (ACCELEROMETER LOOP GAIN) = 23
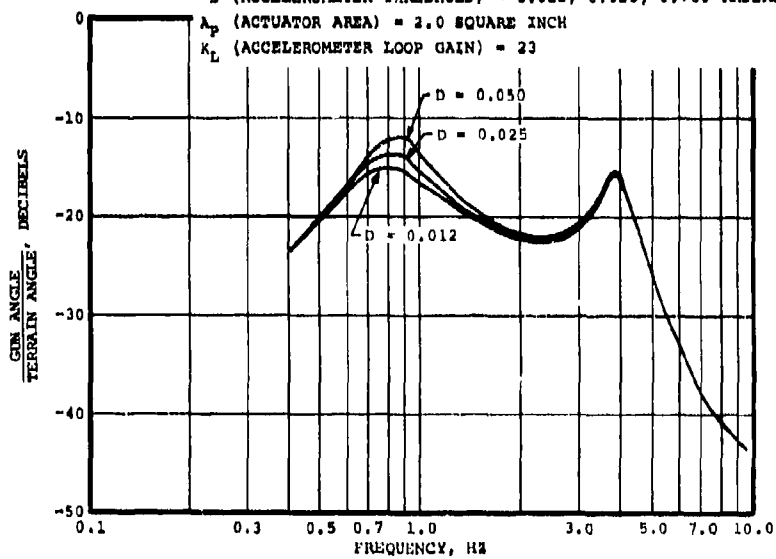
FIGURE 10

DISTURBANCE SUPPRESSION WITH
GUN STABILIZATION SYSTEM

18
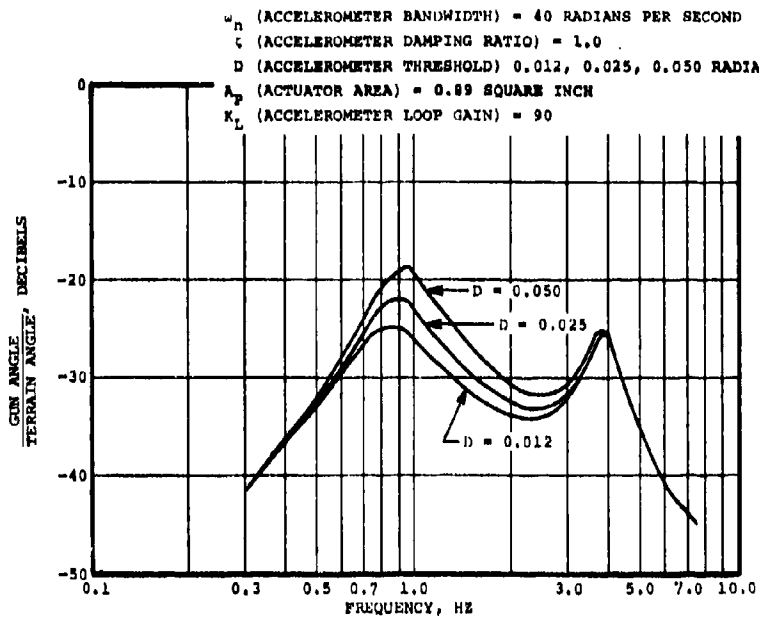
FIGURE 11

DISTURBANCE SUPPRESSION WITH
GUN STABILIZATION SYSTEM
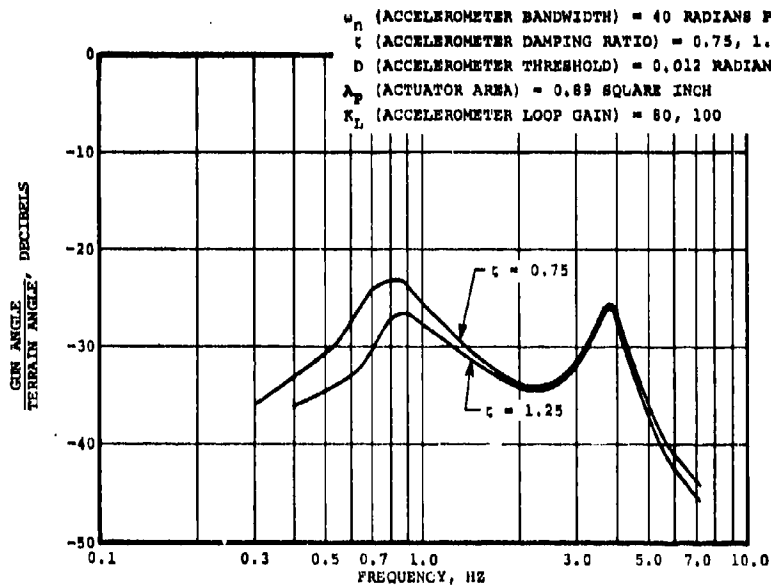
FIGURE 12

DISTURBANCE SUPPRESSION WITH
GUN STABILIZATION SYSTEM

19
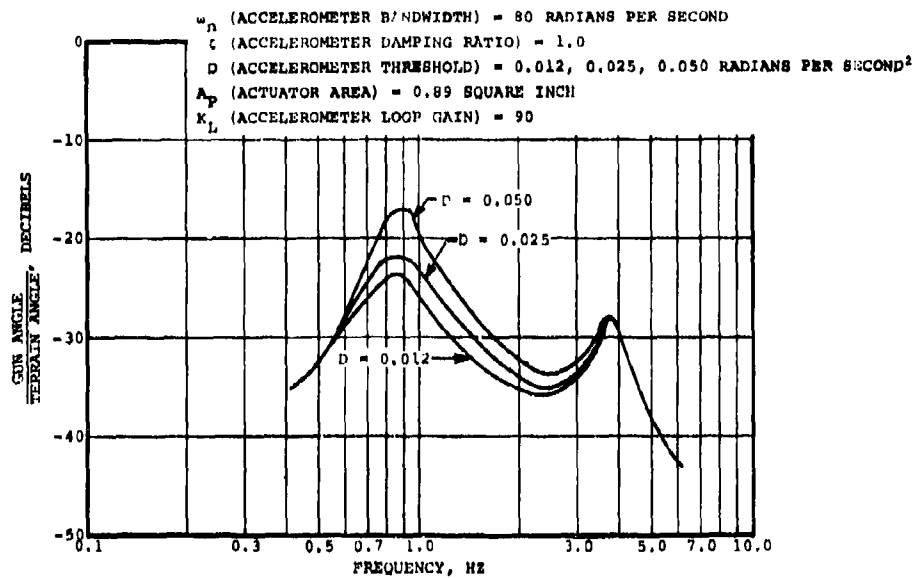
FIGURE 13

DISTURBANCE SUPPRESSION WITH
GUN STABILIZATION SYSTEM
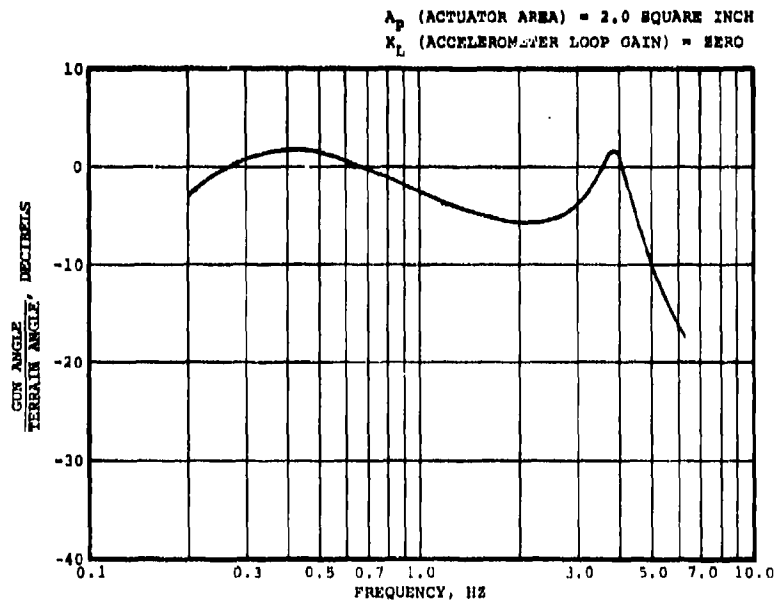
FIGURE 14

DISTURBANCE SUPPRESSION WITHOUT
GUN STABILIZATION SYSTEM (GUNNER ONLY)

20

Figures 15 and 16 show suppression of gun motion in the time domain in response to sinusoidal and step disturbances in the terrain. The effect of the underdamped hull suspension system in amplifying hull motion at frequencies near its resonance point is noted. It is also noted that the system enters a one Hz limit cycle when subjected to low frequency or no terrain disturbances. This is the primary detrimental effect of accelerometer threshold. If the threshold is increased to 0.05 radian per second^2, the limit cycle amplitude increases to 0.003 radian.

A comparison of the gun motion in response to a step change in target position, as exhibited in Figure 17, to the gun motion in Figure 16 demonstrates the necessity of the derivative gunner handle pickoff. Without this handle rate signal to suppress the accelerometer feedback signal, the gunner finds it very difficult to change the gun rate to seek a new target position, and gun response is very slow and sluggish.

2.3.3 Recommendations Based on Analysis - The parameters most affecting suppression of terrain disturbances appear to be accelerometer threshold and actuator time constant. Suppression is not improved by increasing accelerometer bandwidth beyond that necessary to suppress disturbances at the natural frequency of the hull suspension system.

Because of the relation between bandwidth and threshold, it is recommended that the design bandwidth be set at a value of approximately 40 radians per second. Because of the effect of actuator piston area on disturbance suppression, it is recommended that the piston area be reduced to 0.89 square inch. This results in a value of τ_G of 0.7 second.

It is recommended that a handle rate pickoff be included in the system. The response of the pneumatic/hydraulic servovalve should be less than 0.01 second. Accelerometer damping should be at least critical.

3. CONTROLLER DESIGN

A schematic diagram of the controller circuit is presented in Figure 18. The controller utilizes a pneumatic medium for sensing and processing inputs from the gunner's handle and from the accelerometer. The resulting pneumatic output is converted to a hydraulic signal by the pneumatic/hydraulic servovalve. The components of the controller furnished by AiResearch were the accelerometer, handle rate pickoff, and fluidic signal processing circuit. The gunner's handle, servovalve, and actuator were furnished by the U.S. Army (Rock Island Arsenal).

Photographs of the assembled controller and gunner's handle are presented in Figures 19, 20, and 21.

θ_B

0.04
0.02
0
-0.02
-0.04

TERRAIN ANGLE (θ_B), RADIANS

θ_H

-0.04
-0.02
0
0.02
0.04

HULL ANGLE (θ_H), RADIANS

θ_T

0.04
0.02
0
-0.02
-0.04

TARGET ANGLE (θ_T), RADIANS

$\rightarrow$ $\leftarrow$ ONE SECOND

ω_n = 40 RADIANS PER SECOND
ζ = 1.0
D = 0.0125 RADIANS PER SECOND^2
A_p = 0.89 SQUARE INCH
K_L = 90

θ_G

-0.04
-0.02
0
0.02
0.04

GUN ANGLE (θ_G), RADIANS

$\dot{\theta}_G$

0.1
0
-0.1

GUN RATE, ($\dot{\theta}_G$) RADIANS PER SECOND

$\ddot{\theta}_G$

-2
-1
0
1
2

GUN ACCELERATION ($\ddot{\theta}_G$), RADIANS PER SECOND^2

$\ddot{\theta}_P$

1
2
0
-1
-2

ACCELEROMETER OUTPUT ($\ddot{\theta}_P$), RADIANS PER SECOND^2

FIGURE 15

TIME RESPONSE TO SINUSOIDAL TERRAIN

22

ONE SECOND

Θ_B

TERRAIN ANGLE (θ_B), RADIANS

Θ_H

HULL ANGLE (θ_H), RADIANS

Θ_T

TARGET ANGLE (θ_T), RADIANS

ω_n = 40 RADIANS PER SECOND
ζ = 1.0
D = 0.012 RADIAN PER SECOND^2
Λ_p = 0.89 SQUARE INCH
K_L = 90

Θ_G

GUN ANGLE (θ_G), RADIANS

$\ddot{\Theta}_G$

GUN RATE ($\dot{\theta}_G$), RADIANS PER SECOND

$\ddot{\Theta}_G$

GUN ACCELERATION ($\ddot{\theta}_G$), RADIANS PER SECOND^2

$\ddot{\Theta}_F$

ACCELEROMETER OUTPUT ($\ddot{\theta}_F$), RADIANS PER SECOND^2
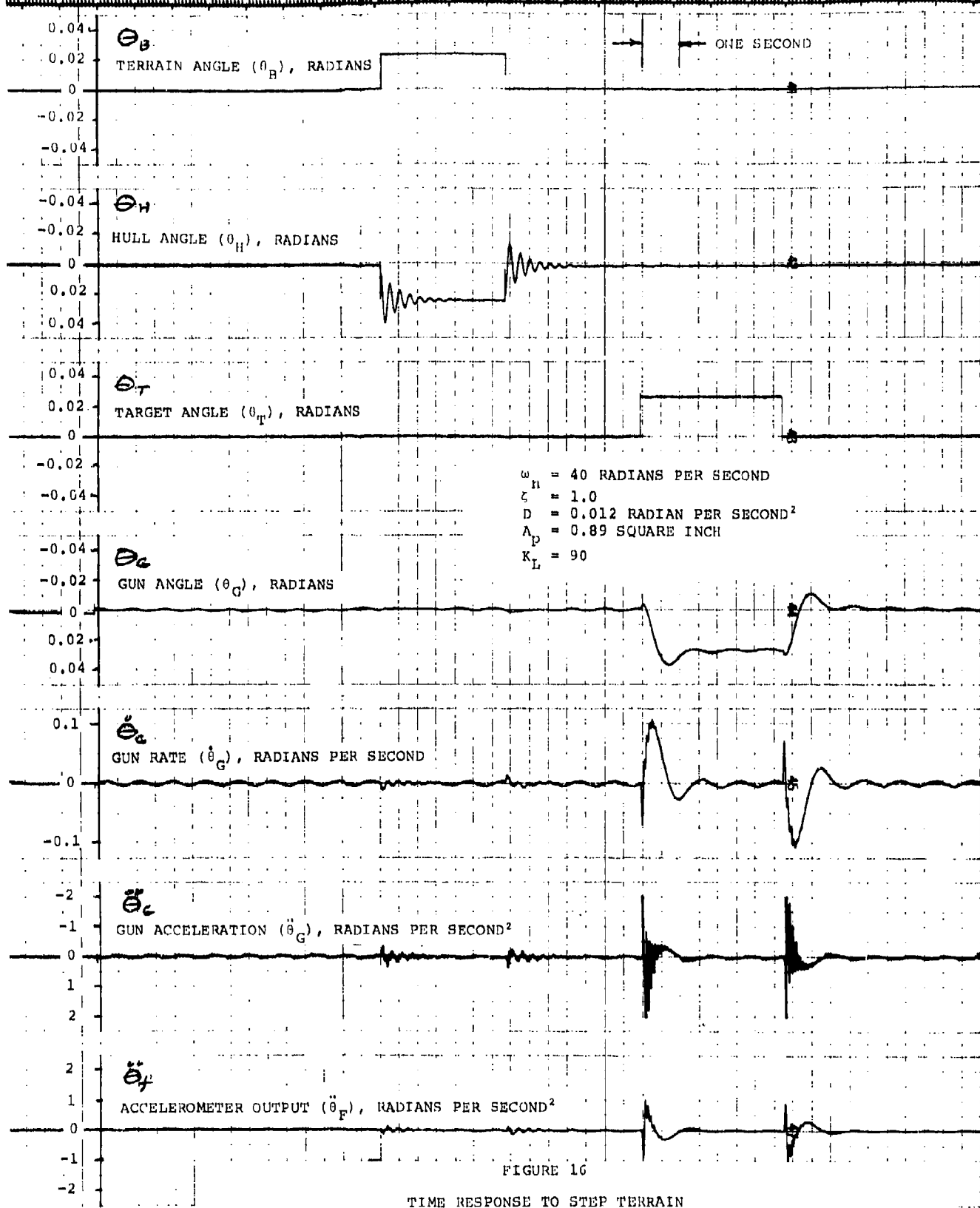
FIGURE 16

TIME RESPONSE TO STEP TERRAIN
AND STEP TARGET

23

θ_B

TERRAIN ANGLE (θ_B), RADIANS

ONE SECOND

θ_H

HULL ANGLE (θ_H), RADIANS

θ_T

TARGET ANGLE (θ_T), RADIANS

ω_n = 40 RADIANS PER SECOND
ζ = 1.0
D = 0.0125 RADIAN PER SECOND^2
A_p = 0.89 SQUARE INCH
K_L = 90
K_2 = 0

θ_G

GUN ANGLE (θ_G), RADIANS

$\dot{\theta}_G$

GUN RATE ($\dot{\theta}_G$), RADIANS PER SECOND

$\ddot{\theta}_G$

GUN ACCELERATION ($\ddot{\theta}_G$), RADIANS PER SECOND^2

$\ddot{\theta}_F$

ACCELEROMETER OUTPUT ($\ddot{\theta}_F$), RADIANS PER SECOND^2
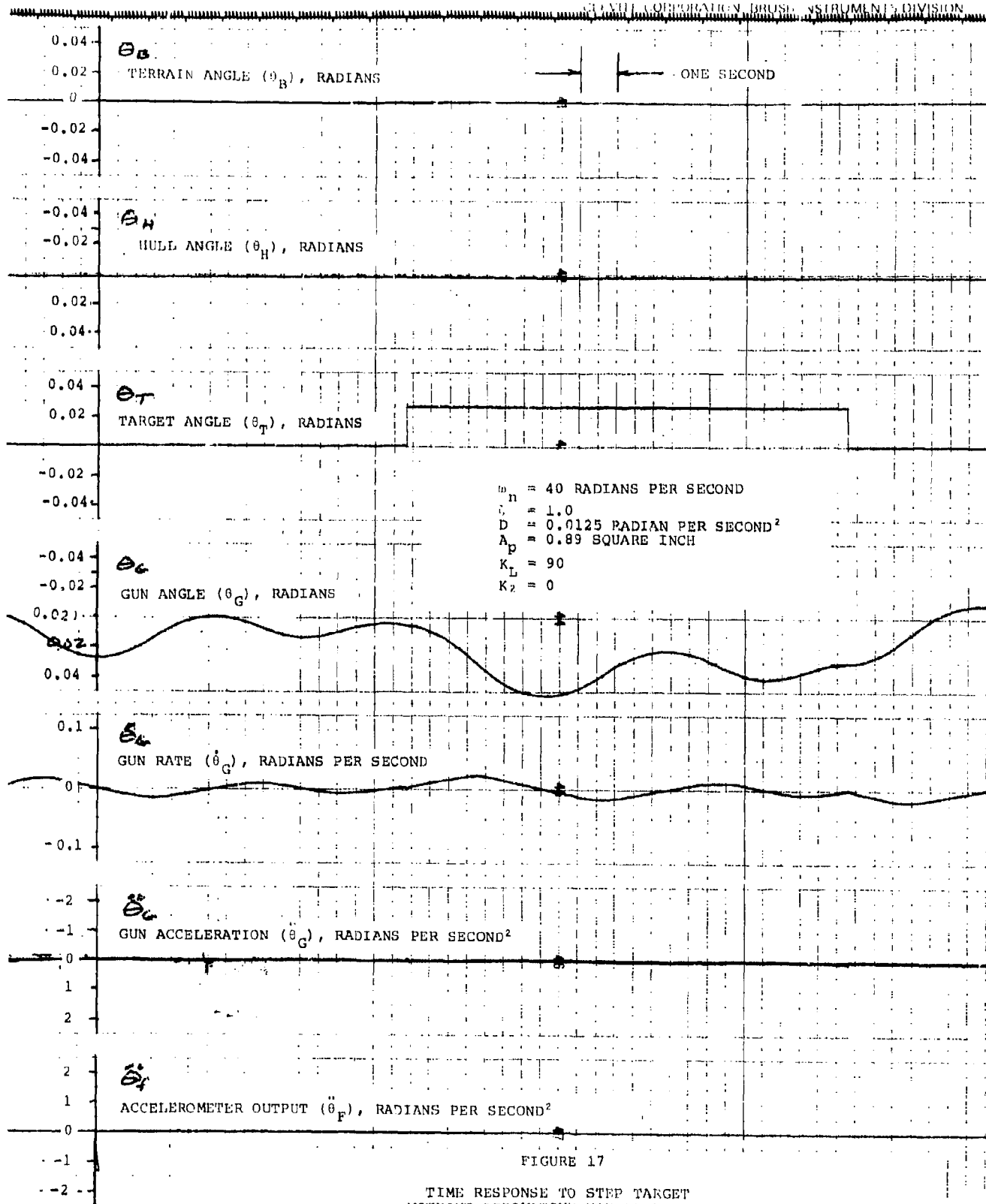
FIGURE 17

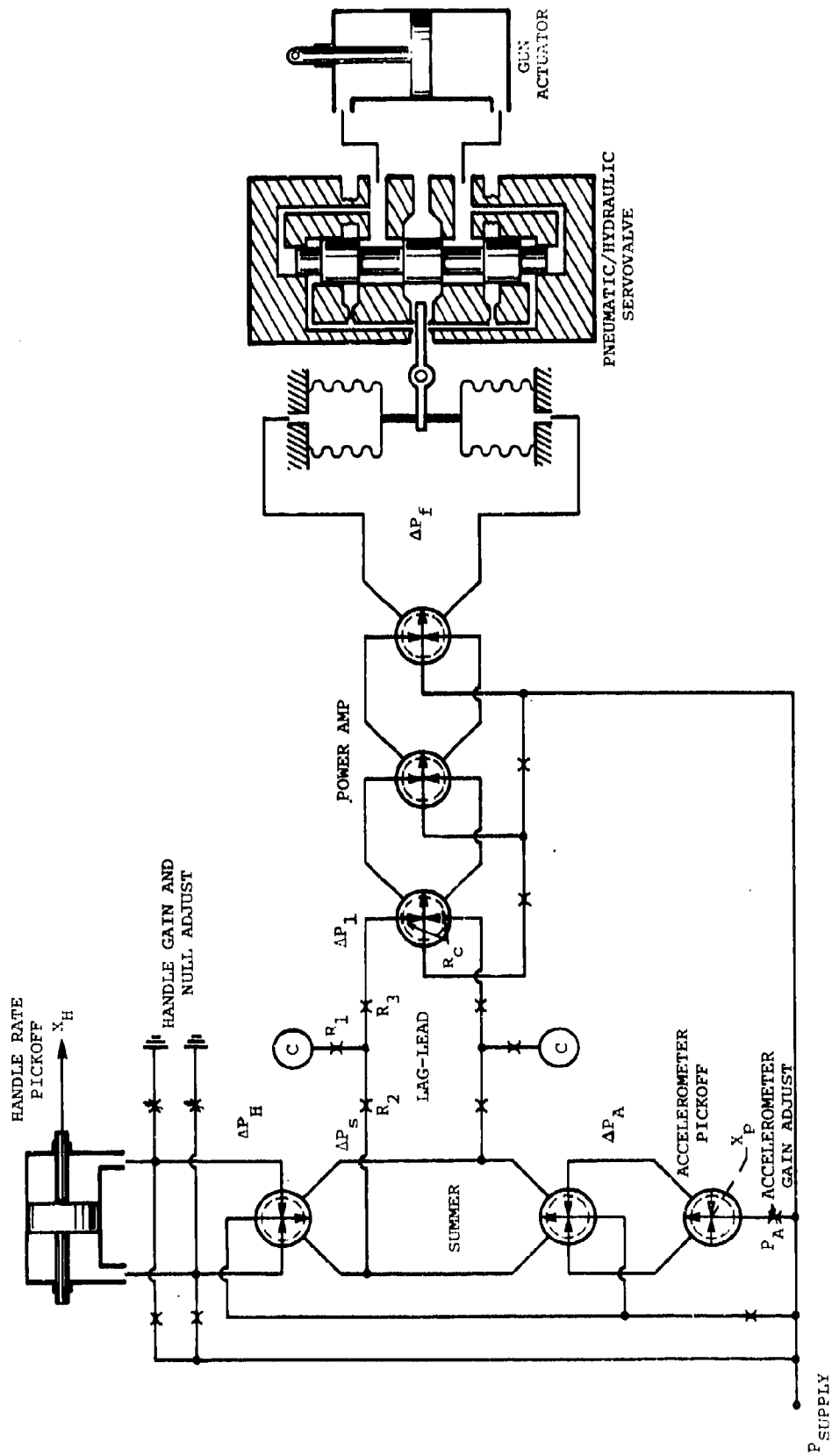TIME RESPONSE TO STEP TARGET
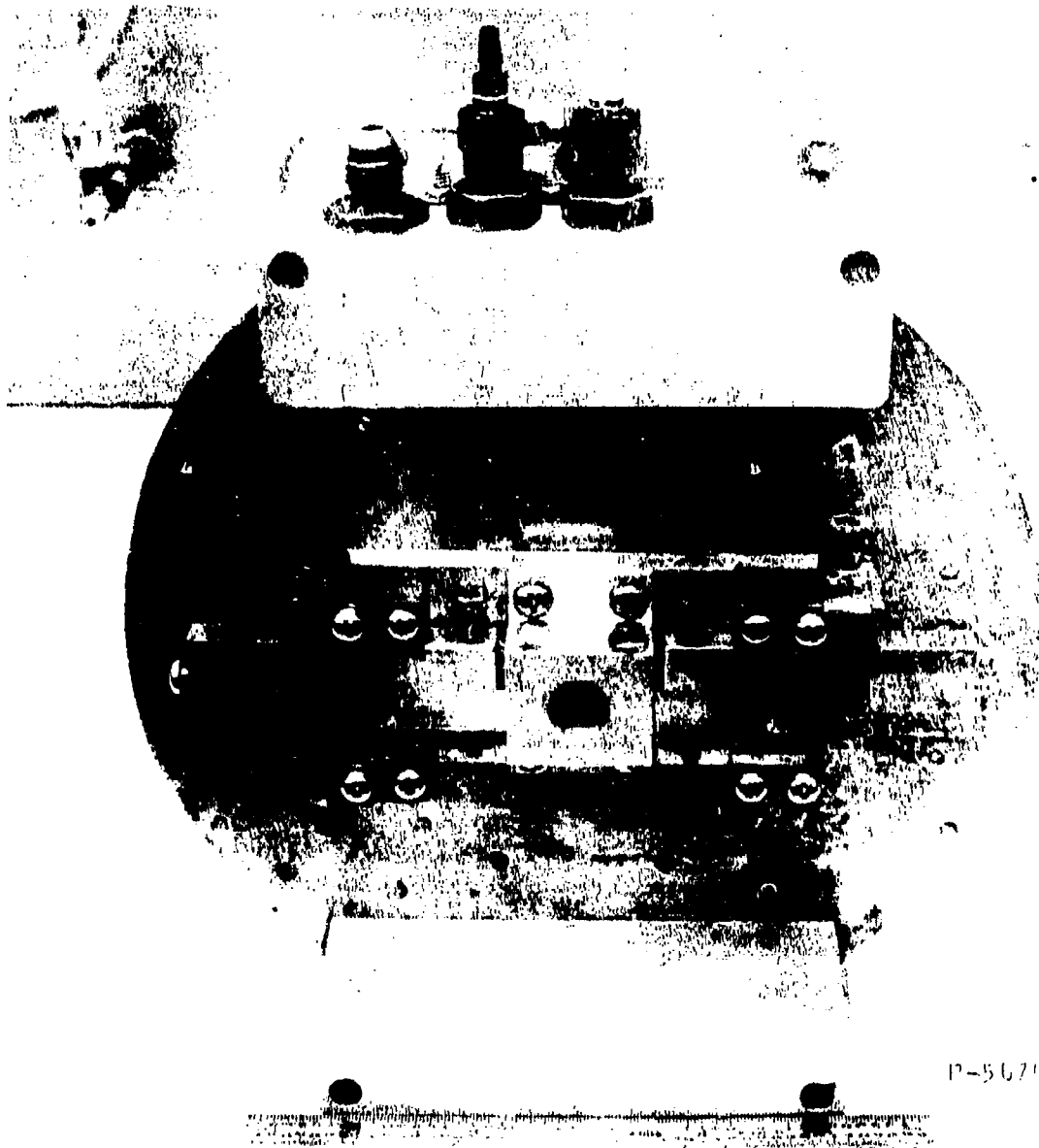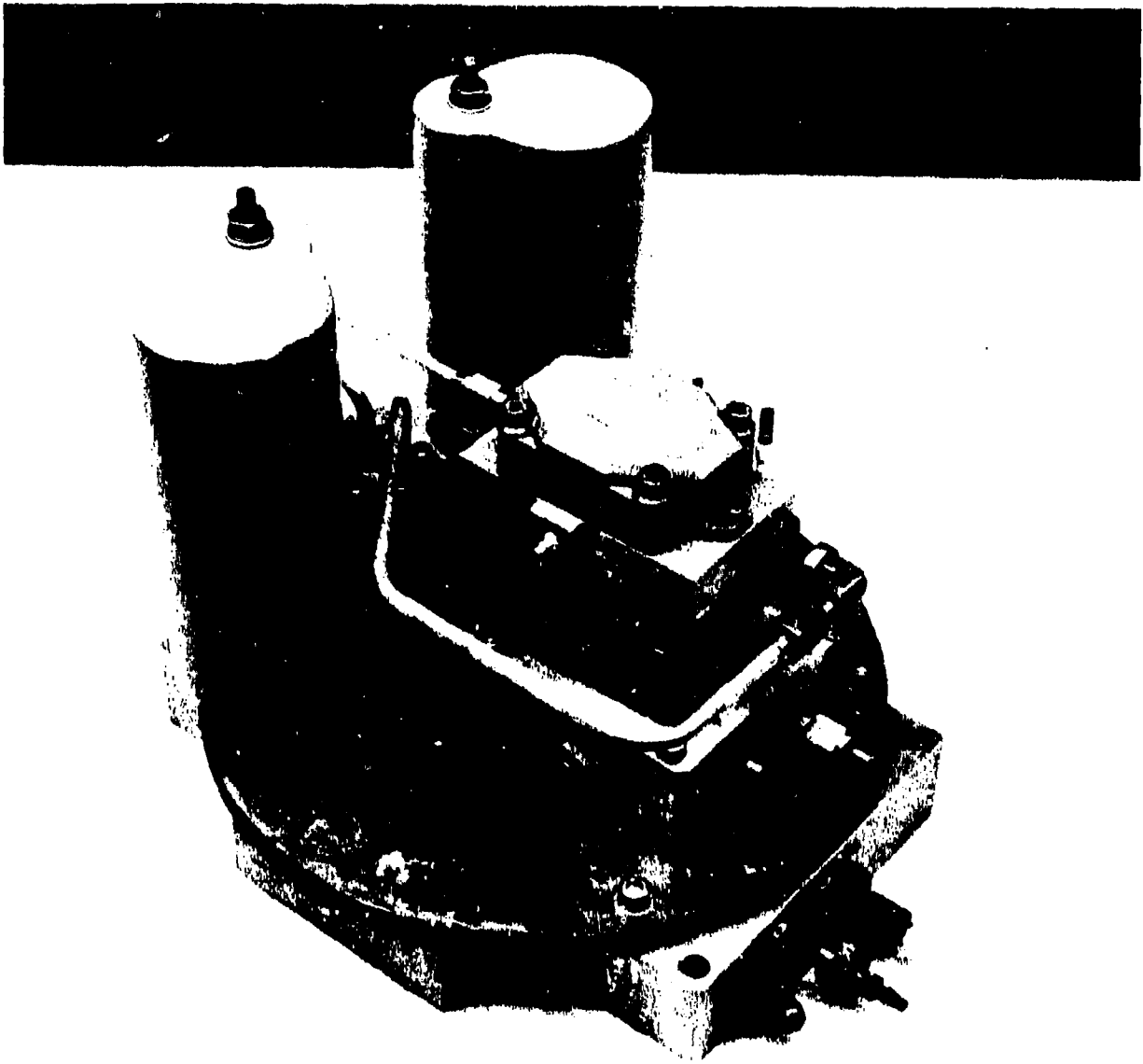WITHOUT DERIVATIVE HANDLE PICKOFF

24

FIGURE 18

FLUIDIC CONTROLLER CIRCUIT

P-5670-5

FIGURE 19

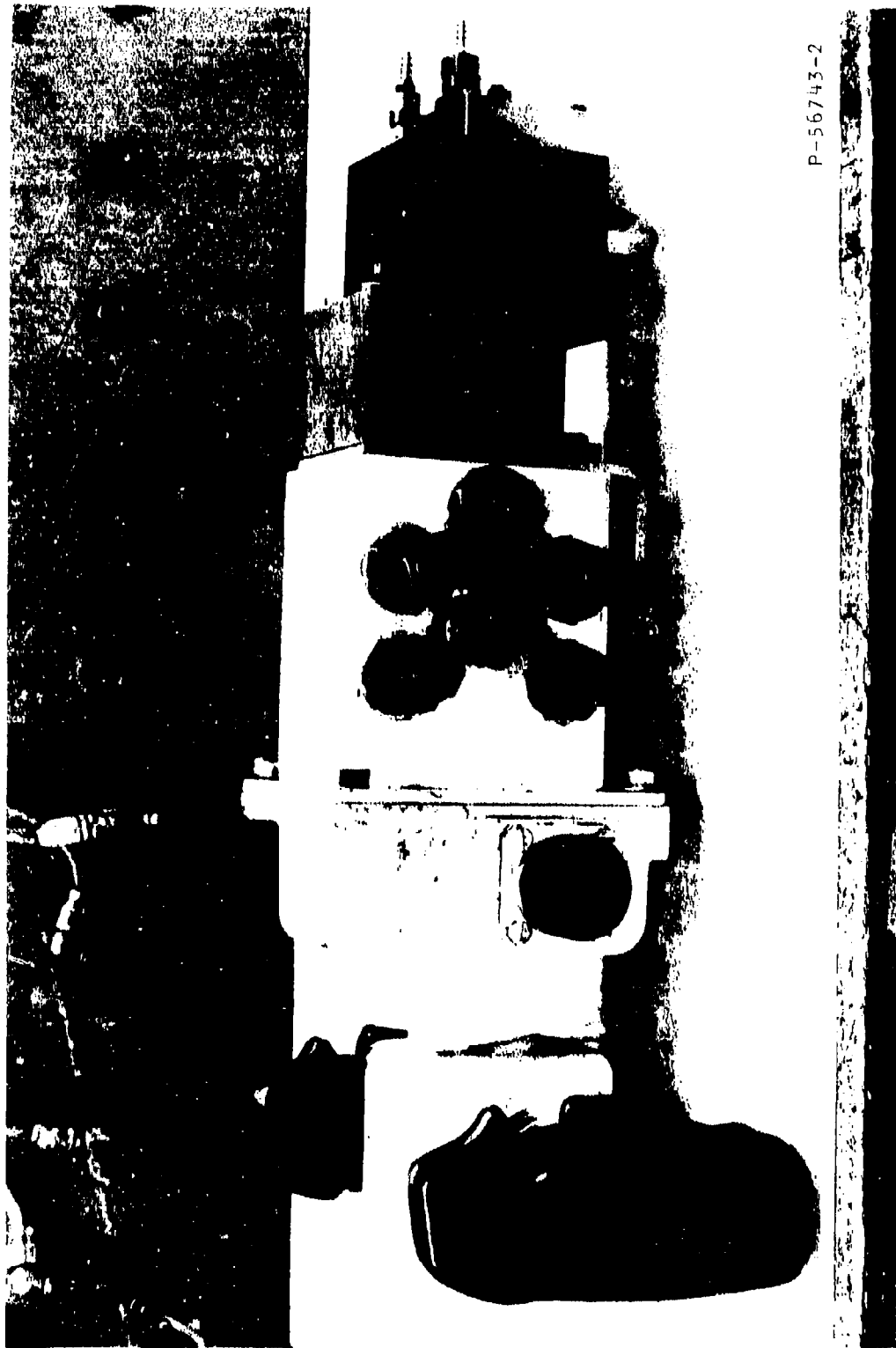HDL FLUIDIC GUN STABILIZATION SYSTEM
(ACCELEROMETER SIDE)

26

P-56743-3

FIGURE 20

HDL FLUIDIC GUN STABILIZATION SYSTEM
(CONTROLLER SIDE)

27

P-56743-2

FIGURE 21

HANDLE VALVE MODIFICATION
HDL FLUIDIC GUN STABILIZATION SYSTEM

3.1 Controller Equation

To obtain a practical specification for the accelerometer-controller unit, the block diagram shown in Figure 1 was reduced by the steps shown in Figure 22. The final block diagram represents the fluidic accelerometer-controller unit developed by AiResearch. The unit receives the inputs of gun acceleration, $\ddot{\theta}_G$, and handle valve position, X_H, and produces a pneumatic output, ΔP_f, to be applied to the servovalve. Using the values listed in Figure 1, the input-output relation for the device is determined from the block diagram to be as follows:

$$\Delta P_f = \left[0.1572\ K_L\ \frac{S^2\ \theta_G}{\frac{S}{49}^2 + \frac{25}{49} + 1} + 0.3743\ K_L\ \frac{SX_H}{1 + 0.05S} \right] X$$

$$\left[\frac{1 + 0.05S}{(1 + 2S)(1 + 0.01S)} \right]$$

As outlined in Appendix B, the accelerometer transfer function is computed to be

$$X_P = \frac{r}{\omega_n^2}\ \frac{\ddot{\theta}_G}{\frac{S^2}{\omega_n^2} + 2\ \frac{\zeta S}{\omega_n} + 1}$$

$$X_P = (1.25 \times 10^{-3})\ \frac{S^2\ \theta_G}{\frac{S^2}{\omega_n^2} + 2\ \frac{\zeta S}{\omega_n} + 1}\ \text{inches,}$$

where X_P is the displacement input to the pin amplifier pickoff.

The equation describing the fluidic controller circuit is then:

$$\Delta P_f = \left(125.76\ K_L X_P + 0.3743\ K_L\ \frac{SX_H}{1 + 0.05\ S} \right)\ X$$

$$\left(\frac{1 + 0.05\ S}{(1 + 2\ S)(1 + 0.01\ S)} \right)\ \text{psid.}$$
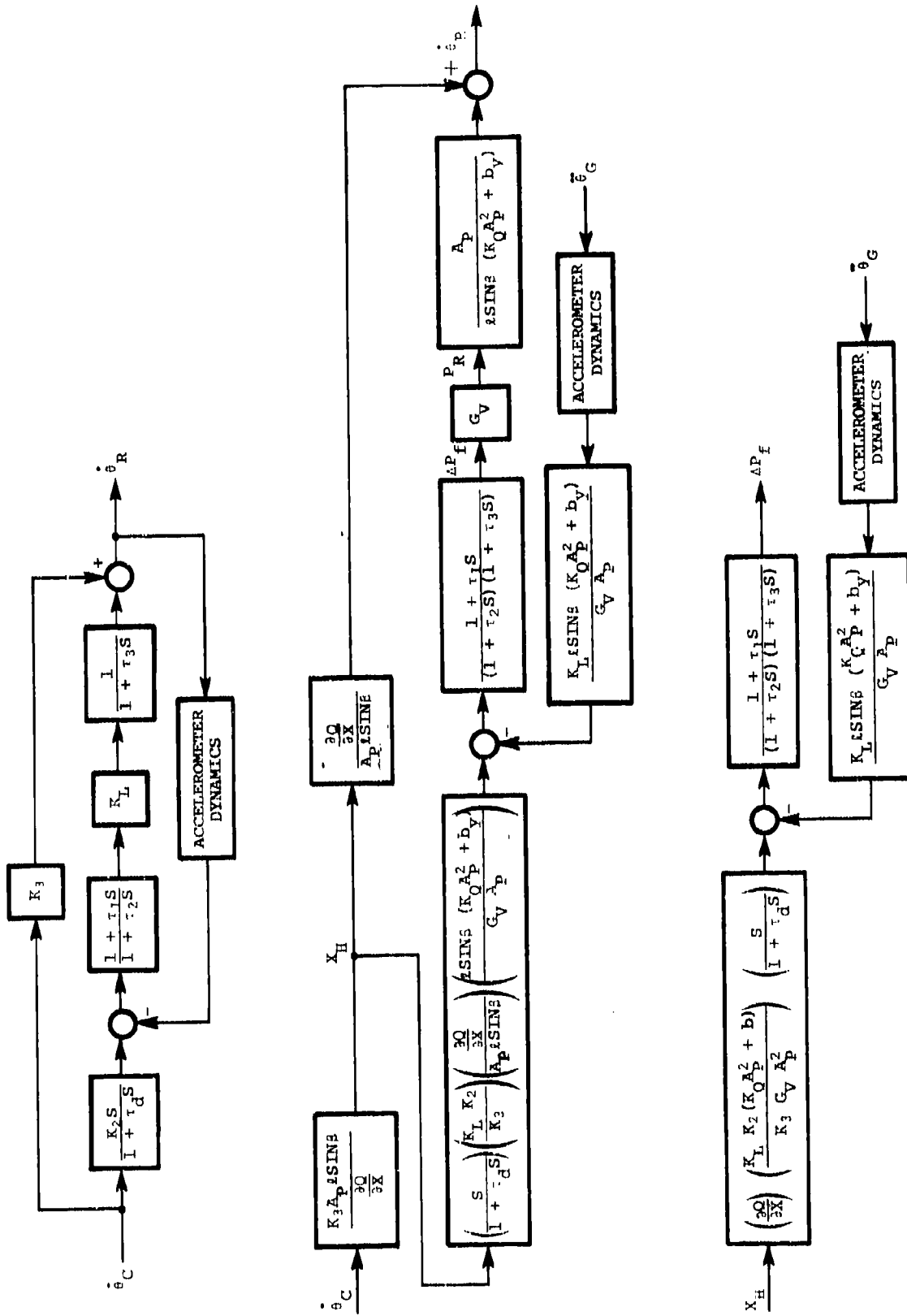
29

FIGURE 22

DERIVATION OF ACCELEROMETER CONTROLLER
BLOCK DIAGRAM

30

3.2 Accelerometer

As shown in Figure 23, the accelerometer consists of a rectangular proof mass suspended at the center of mass by a rotational spring flexure. Motion of the mass relative to its housing is sensed by a pin amplifier which measures the relative displacement of the end of the proof mass. The mass is provided with balancing screws to place the center of mass precisely at the center of rotation. This minimizes the sensitivity of the accelerometer to linear accelerations.

The pin amplifier, in its present state of development, has a resolution of approximately 2×10^{-6} inches. This corresponds to an acceleration resolution of 1.71×10^{-3} radians per second^2, which is considered adequate for suppressing gun motions to an amplitude approximately 25 db down from hull disturbance inputs.

Motion of the proof mass is damped by a magnetic fluid suspended by a pair of cylindrical magnetic pole pieces protruding into cylindrical cavities in the proof mass, forming a squeeze film. This mechanism has been found to provide an excellent method of damping for breadboard and feasibility demonstration components, primarily because of its adjustability. The nature of the presently available diester base magnetic fluid may preclude its use in a production system unless further improvements are made in this fluid. Two properties of this fluid cause concern: (a) the temperature-viscosity properties may limit the temperature range over which system operation is satisfactory, and (b) the volatility of the fluid will limit the operational and shelf life of the system. For these reasons, alternate methods of accelerometer damping are required.

The rotational spring flexure which was used in the breadboard units is a commercially available device commonly used in many instrument designs. Information which is available on this flexure design indicates that cross-axis sensitivity of the accelerometer could be improved by substitution of a cruciform design flexure. The cruciform design was developed by AiResearch for an electrofluidic transducer designed for use in a severe shock environment. The cruciform flexure exhibits the high cantilever/rotational spring rate ratio necessary for reduction of cross-axis sensitivity. In addition, there is greater design flexibility and a significant cost advantage in the use of this flexure. The cruciform design will be investigated further for any two-axis stability system that may be developed.
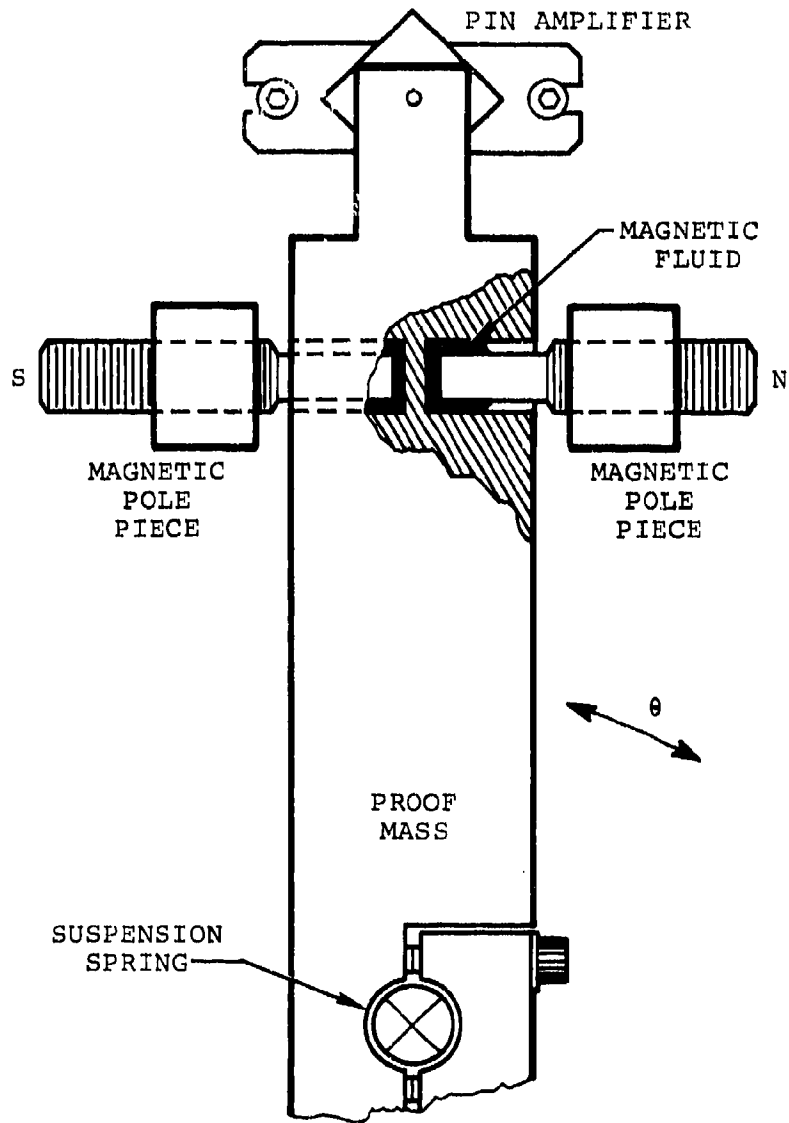
31

FIGURE 23

FLUIDIC ACCELEROMETER FOR
GUN STABILIZATION SYSTEM

3.3 Fluidic Controller Circuit

The controller circuit was built in accordance with the schematic diagram in Figure 18. The circuit operates with a supply pressure of 2.0 psig and the output pressure, ΔP_f, has a range of ± 1.0 psid.

The lag-lead dynamic compensation is performed by the resistance-capacitance network and is governed by the relation

$$\frac{\Delta P_\ell}{\Delta P_S} = \left(\frac{R_C}{R_2 + R_3 + R_C} \right) \left[\frac{1 + R_1 \ CS}{1 + \left(R_1 + \frac{R_2 R_3 + R_2 R_C}{R_2 + R_3 + R_C} \right)(CS)} \right]$$

A lag time constant of approximately 2.0 seconds was obtained with a volume of 17 cubic inches and four laminations of capillary resistor (AiResearch Part 3155026) serving as R_2 and R_3. The resistance, R_1, needed to obtain a lead time constant of 0.05 second is the approximate resistance of the transfer passage to the volumes through the fluidic stack.

The handle rate pickoff signal is summed with the accelerometer pin amplifier signal by means of impedance summing, utilizing the output impedances of the amplifiers.

After the summed signal is processed by the lag-lead network, it is amplified by a three-stage cascade to the required pressure gain and to the required power level to drive the input bellows of the servovalve. Amplifiers of a new HDL design, AiResearch Part 3155131, which is superior in both noise and gain characteristics, were used throughout.

3.4 Handle Rate Pickoff

The handle rate signal was obtained from a small double-acting piston which was installed on the handle valve. The piston shaft was spring-loaded against the end of the valve spool so that the piston moved with the spool. The chambers on either side of the piston are connected to the control ports of a fluidic amplifier (refer to Figure 18). The relation between the piston displacement, X_H, and the amplifier input differential, ΔP_H, is given by the expression on the following page.

$$\Delta P_H = \left(\frac{2\ R\ A_H\ \overline{P}_H}{R_g\ T}\right) \left(\frac{S}{R\ C_H\ S\ +\ 1}\right) \left(X_H\right)$$

where

R is the combined resistance of the amplifier control ports and nulling orifices,

A_H is the piston area,

$\overline{P}_H$ is the average absolute pressure in the piston chambers,

C_H is the pneumatic capacitance of the piston chambers,

X_H is the piston displacement,

R_g is the gas constant for air, and

T is the absolute air temperature.

4. TEST PROGRAM

The tests conducted on the fluidic gun stabilization system and components included the following:

○ Bench testing of controller and components

○ Determination of open loop dynamic characteristics

○ Closed loop disturbance suppression

The following paragraphs describe each of these test areas.

4.1 Bench Testing

4.1.1 Gunner's Handle Valve - A flow test was conducted on the handle valve to determine flow area versus valve displacement. This information was needed to properly scale the handle rate

34

pickoff signal. The valve was connected as shown in Figure 24 and supplied with MIL-H-5606 hydraulic oil at a pressure of 500 psi. This was the maximum capability of the bench pump at the required flow rate. The flow rate was measured downstream of the valve before entering the sump, using a turbine flowmeter with digital readout.
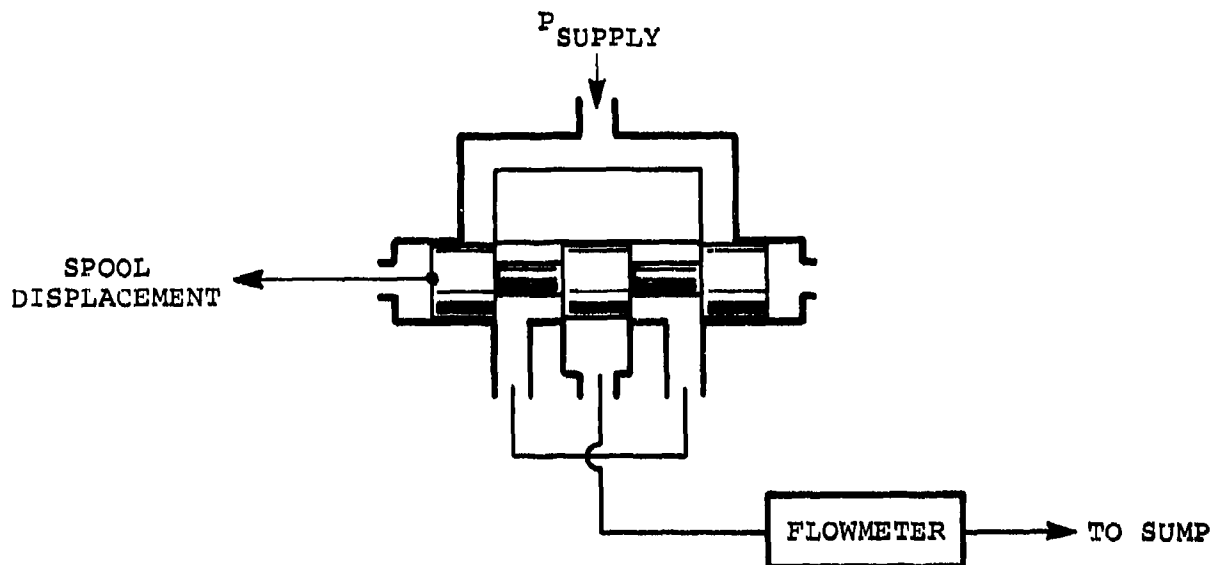

FIGURE 24

TEST SETUP FOR
HANDLE VALVE FLOW TEST

The results of the flow test are plotted in Figure 25. Since flow values between ±0.05 gpm could not be measured with the available flowmeter, the shape of the curve as it passes through the zero point is estimated.

4.1.2 Accelerometer-Controller Circuit - Dynamic testing of the accelerometer was performed on an oscillating angular rate table which was specially constructed for this program. The table, shown in Figure 26, was capable of oscillating at amplitudes of from 0.005 to 1.0 radian per second over a frequency range from zero to 15 Hz.
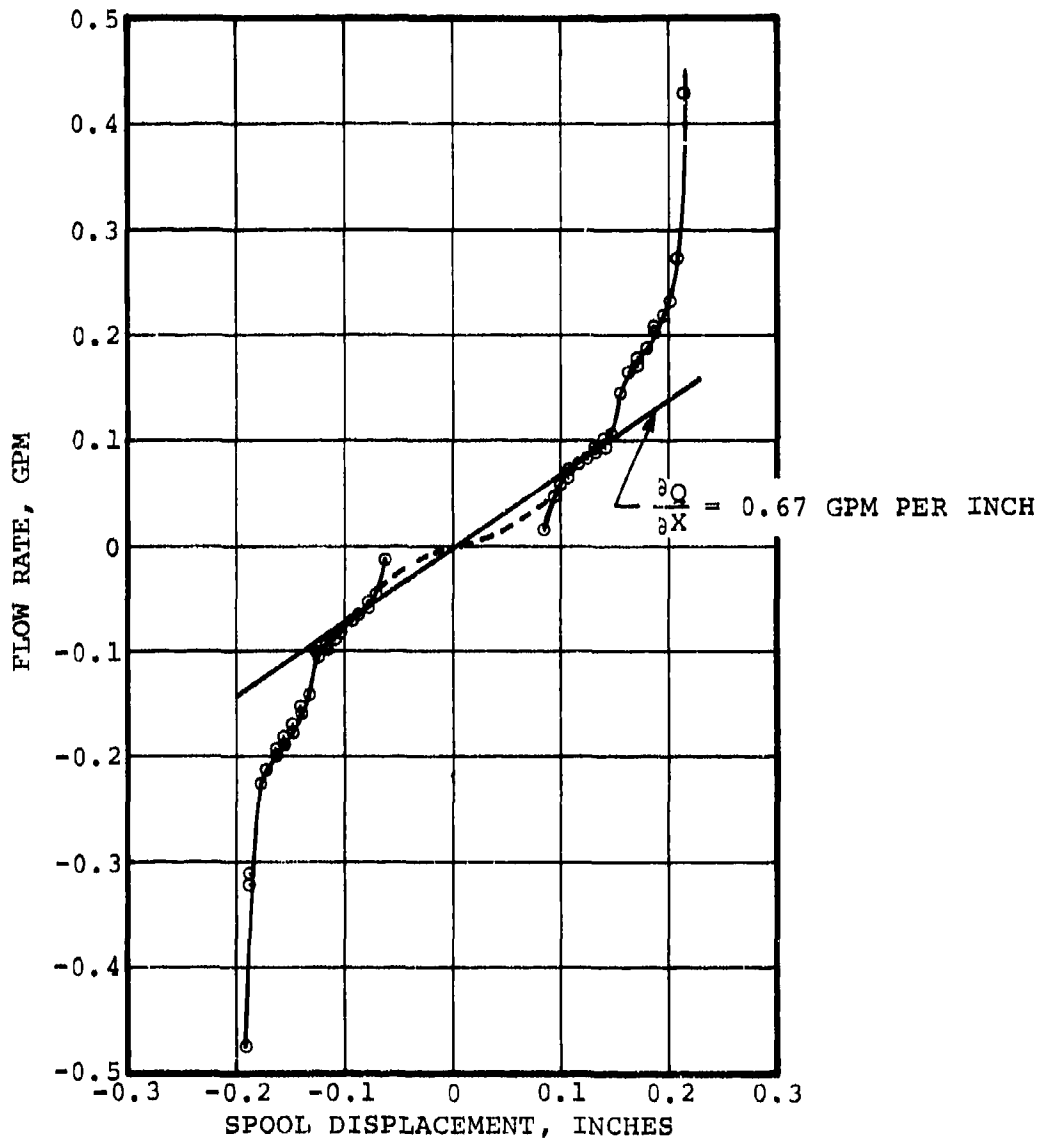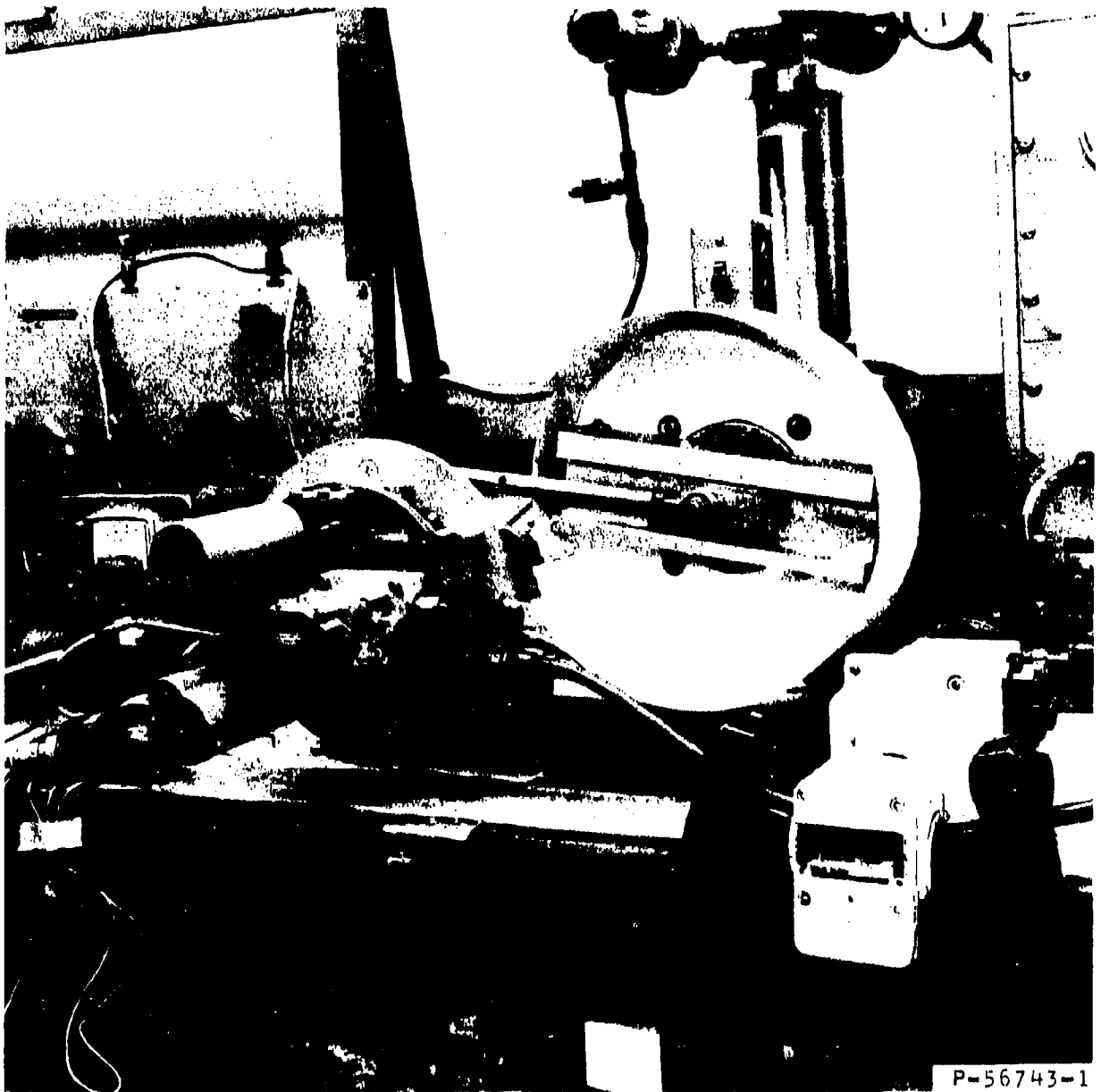
35

FIGURE 25

HANDLE VALVE FLOW
VERSUS SPOOL POSITION

36

P-56743-1

OSCILLATING ANGULAR RATE TABLE
HDL FLUIDIC GUN STABILIZATION SYSTEM PROGRAM

FIGURE 26

MP-57252

Difficulty was encountered during dynamic testing of the
accelerometer over the full frequency range because of rumble
and backlash in the test fixture. Valid data was extracted only
at low frequencies and at fairly large oscillation amplitudes.
The data obtained, together with the plotted design performance,
is presented in Figure 27. It is noted that good agreement was
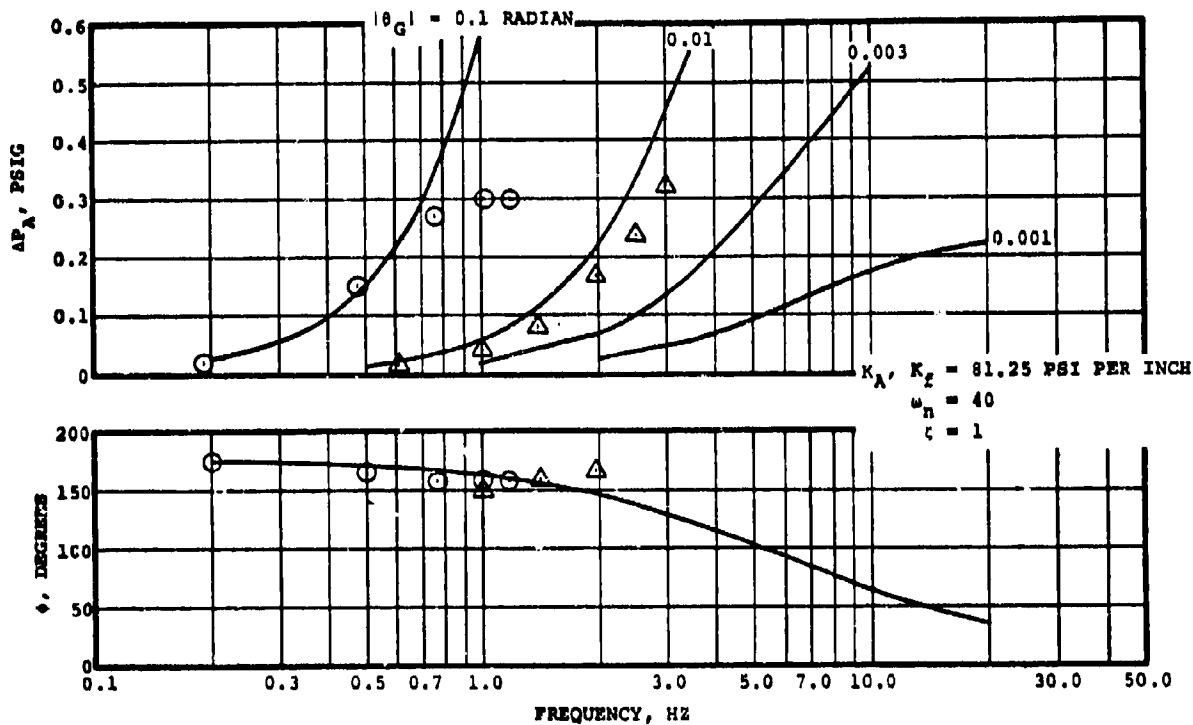obtained when the oscillation amplitude, $|\theta_G|$, was set at
0.1 radian.

FIGURE 27

PERFORMANCE OF ACCELEROMETER
FOR GUN STABILIZATION SYSTEM

38

To circumvent the necessity for testing the controller on the accelerometer test fixture at high frequencies, dynamic testing of the controller circuit was performed by simulating accelerometer inputs with an electrofluidic transducer which contained a pin amplifier identical to the accelerometer pickoff amplifier. The amplitude ratio and phase relationships between fluidic controller output pressure and electrofluidic transducer input current are plotted in Figure 28.

Static performance of the controller circuit was verified by placing the pin amplifier on a fixture which was capable of moving the pin and precisely measuring its position. The output pressure of the controller is plotted versus pin position in Figure 29. Gain of the controller is adjusted by varying the supply pressure to the pin amplifier.

As a check on controller performance and to verify correct operation of the pneumatic/hydraulic servovalve, the controller/servovalve combination was tested on the hydraulic bench. Accelerometer inputs were again simulated with the electrofluidic transducer. The resulting static and dynamic data are plotted in Figures 30 and 31, respectively.

4.2 Open Loop Testing

An open loop frequency response test was performed on the fluidic gun stabilization system to verify the values of system parameters that were used during the analytical phase of the program. The actuation system subjected to test was that installed in the MIC-V turret test fixture located at Rock Island Arsenal. The actuator was powered by the pneumatic/hydraulic pressure control servovalve supplied by the U.S. Army for the program.

As a result of the recommendations presented in paragraph 2.3.3 that the value of τ_G be increased to 0.7 second, the actuator piston area was decreased to 1.2 square inches and the actuator moment arm was decreased to 5.7 inches.

The moment of inertia of the gun was simulated by installing an eight foot length of four inch diameter barstock in the gun cradle. The test setup is shown in Figure 32.
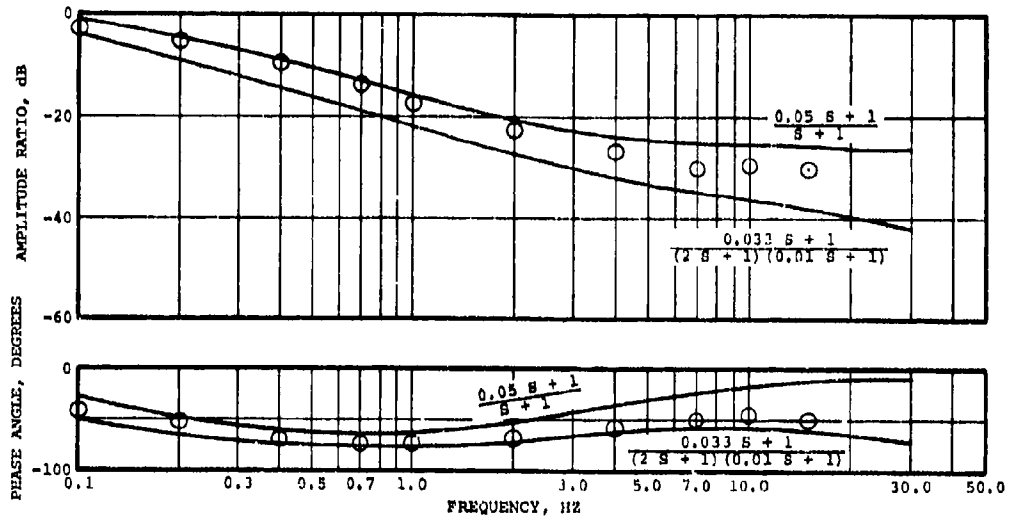
FIGURE 28

FLUIDIC LAG-LEAD RESPONSE FOR
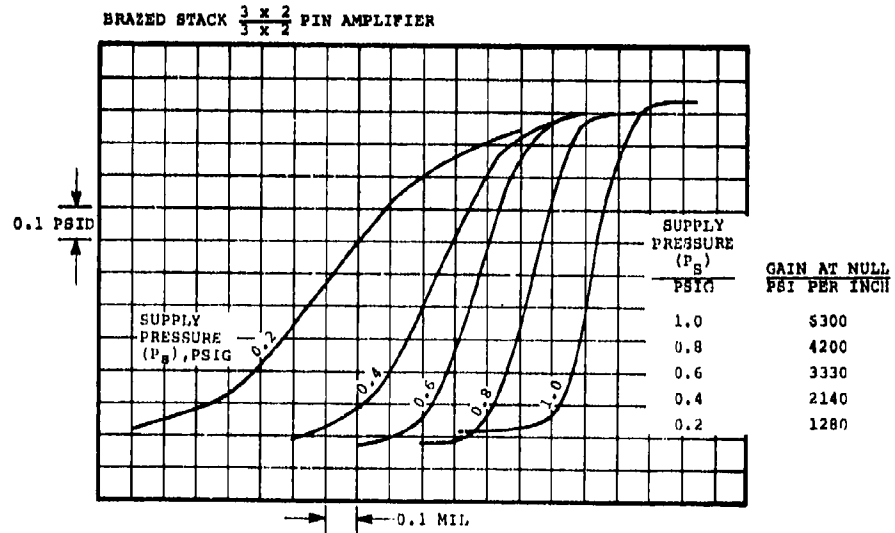GUN STABILIZATION SYSTEM

FIGURE 29

STATIC PERFORMANCE OF
CONTROLLER CIRCUIT

40

400

300

200

100

0

P_L, PSID

-100

-200

-300

-400

-4   -3   -2   -1   0   1   2   3   4

ΔP_A, INCHES OF WATER

ΔP_H

OUTPUT NOISE, PSID

10

0

-10

1.0 SECOND
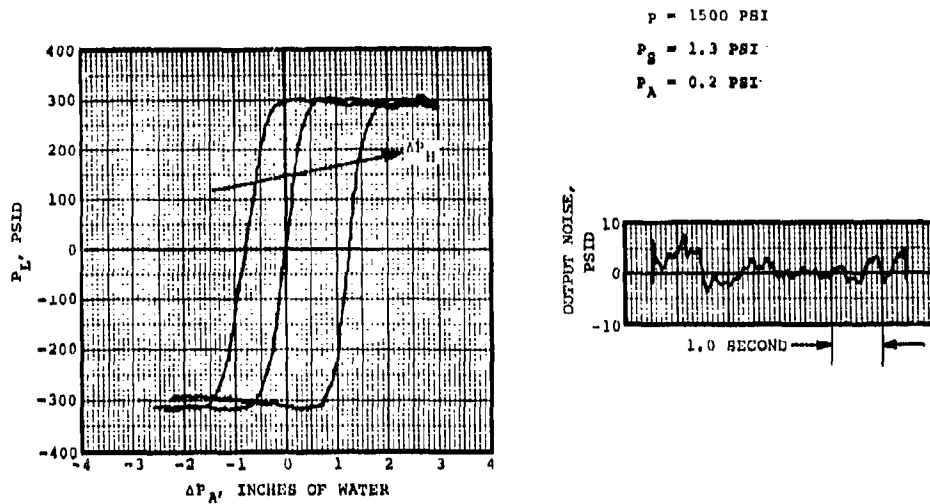
FIGURE 30

STATIC PERFORMANCE OF
CONTROLLER SERVOVALVE
(HYDRAULIC OUTPUT PRESSURE VERSUS
PIN AMPLIFIER OUTPUT PRESSURE)

AMPLITUDE RATIO, DIMENSIONLESS

0.5

0.4

0.3

0.2

0.1

0

$$\frac{1 + 0.05\ S}{(1 + 2\ S)(1 + 0.01\ S)}$$

P_L = 1500 PSI

P_B = 1.3 PSI

P_A = 0.2 PSI

PHASE, DEGREES

0

-100

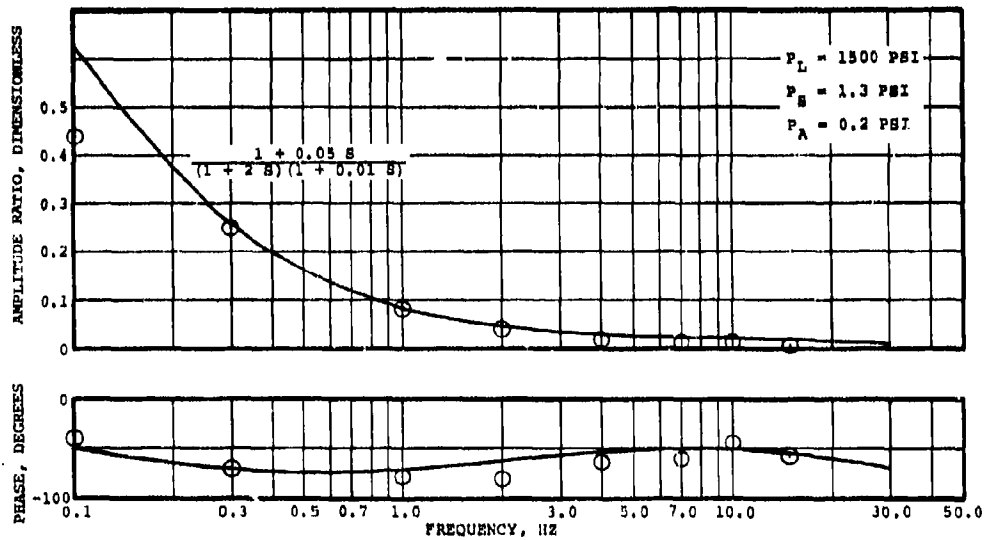0.1   0.3   0.5 0.7   1.0   3.0   5.0 7.0 10.0   30.0   50.0

FREQUENCY, HZ

FIGURE 31

DYNAMIC PERFORMANCE OF
CONTROLLER/SERVOVALVE
(HYDRAULIC OUTPUT PRESSURE VERSUS
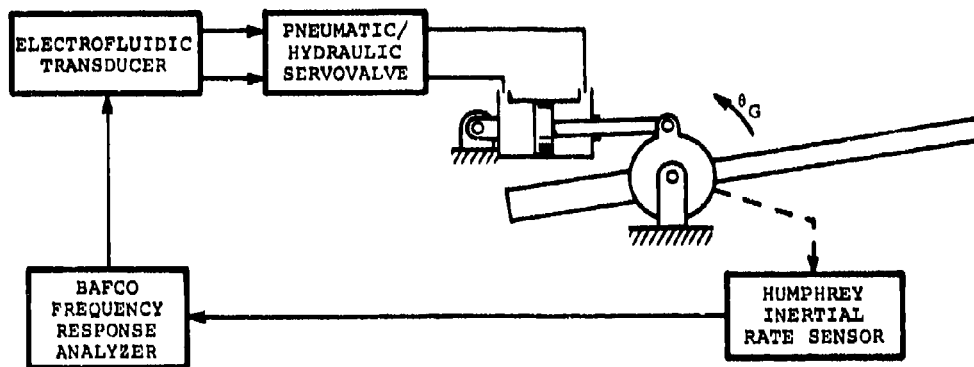ELECTROFLUIDIC TRANSDUCER INPUT CURRENT)

41

FIGURE 32

TEST SETUP FOR OPEN LOOP
FREQUENCY RESPONSE TEST

The angular rate of the gun at various frequencies was
compared to the electrofluidic transducer command signal by
means of the Bafco frequency response analyzer. The results of
this test are plotted in Figure 33.

As evident from the data, the time constant, τ_G, of the
actuation system was 0.16 second rather than the expected value
of 0.7 second and was accompanied by an apparent transport delay
of 0.02 second. This discrepancy was attributed to the presence
of coulomb friction in the system, the value of which was
determined by measurement to be approximately 46 foot-pounds.
If the rate amplitude is assumed to be 0.25 radian per second,
the equivalent friction coefficient, b_y, is determined to be
approximately 68 pound-second per inch instead of the value of
0.15 pound-second per inch which was assumed in the analysis.

4.3 Closed Loop Testing

It was analytically determined that, because of the
discrepancy in the value of the time constant, τ_G, of the
actuation system, performance of the controller as initially
designed would be poor.

Because of the lack of time, it was not possible to make a
major readjustment of the dynamic compensation circuit to accom-
modate the lower value of τ_G. However, analysis showed that
disturbance suppression could be enhanced somewhat at low fre-
quencies (0.1 to 1.0 Hz) by increasing the accelerometer damping
ratio. This is shown in Figure 34. Since this adjustment was
easily implemented, the system was tested under these conditions.

42
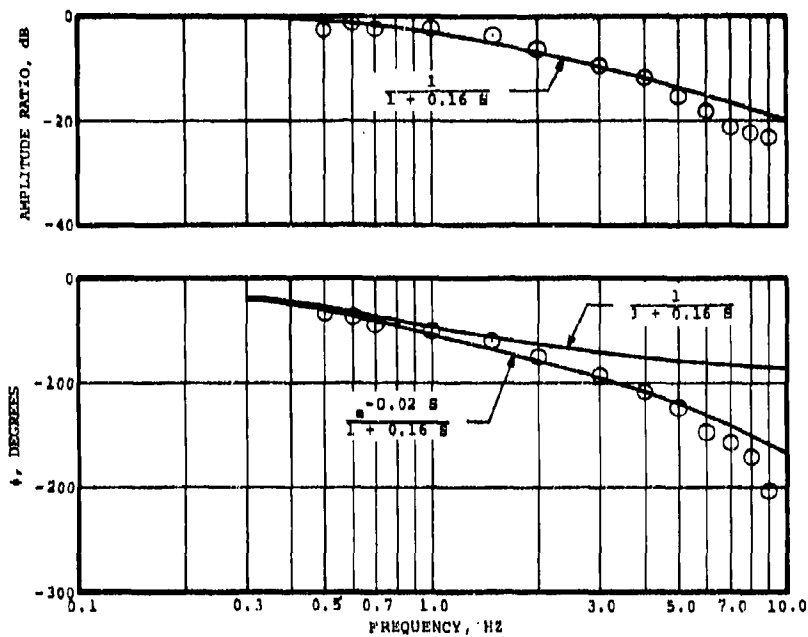
FIGURE 33

GUN RESPONSE TO SERVOVALVE INPUT
(4 INCH DIAMETER X 7 FEET LONG
BARSTOCK IN GUN CRADLE)

τ_G = 0.16 SECOND
TRANSPORT DELAY = 0.02 SECOND
ζ = 5
ω_n = 5.5 HZ
τ_1 = 0.05 SECOND
τ_2 = 2.0 SECOND
τ_3 = 0.01 SECOND

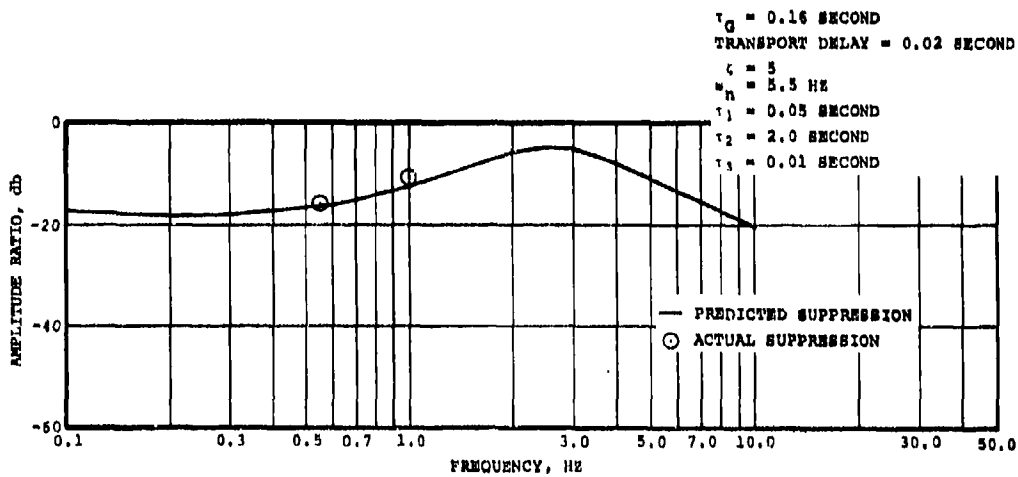—— PREDICTED SUPPRESSION
⊙ ACTUAL SUPPRESSION

FIGURE 34

CLOSED LOOP
DISTURBANCE SUPPRESSION WITH
GUN STABILIZATION SYSTEM

43

The resulting disturbance suppression performance is plotted in Figure 34. Photographs of the turret test fixture and the controller installation are presented in Figures 35 and 36, respectively.

5. CONCLUSIONS AND RECOMMENDATIONS

5.1 Conclusions

The following was accomplished during the program:

○ An analytical method was developed that can adequately predict the performance of a gun stabilization system. The linear frequency response model is of value because of its ability to quickly determine the effects of parameter changes on system performance. The more detailed analog computer model permitted a more precise evaluation of system performance because of its ability to include threshold and saturation non-linearities. The presentation of the analytical results in frequency response form rather than in the form of a step response or a random bump course permits objective comparison of the performance of various system concepts based on overall disturbance suppression performance. Both the linear and analog models can be extended to include more complex plant dynamics such as bending of the gun barrel.

○ An accelerometer-controller unit was designed and fabricated to conform to a predetermined control equation. Advances were made and experience gained in working with pneumatic fluidic elements in the laminar flow regime. Use of a pin amplifier as a position sensing device for the accelerometer proved to be satisfactory. The commercial spring flexure used in the system was suitable for demonstrating system feasibility. However, as anticipated, this device will not be suitable for use in a production system because of the low natural frequency exhibited in a cross-axis direction. Also as anticipated, the magnetic fluid damping mechanism exhibited fairly severe temperature dependence.
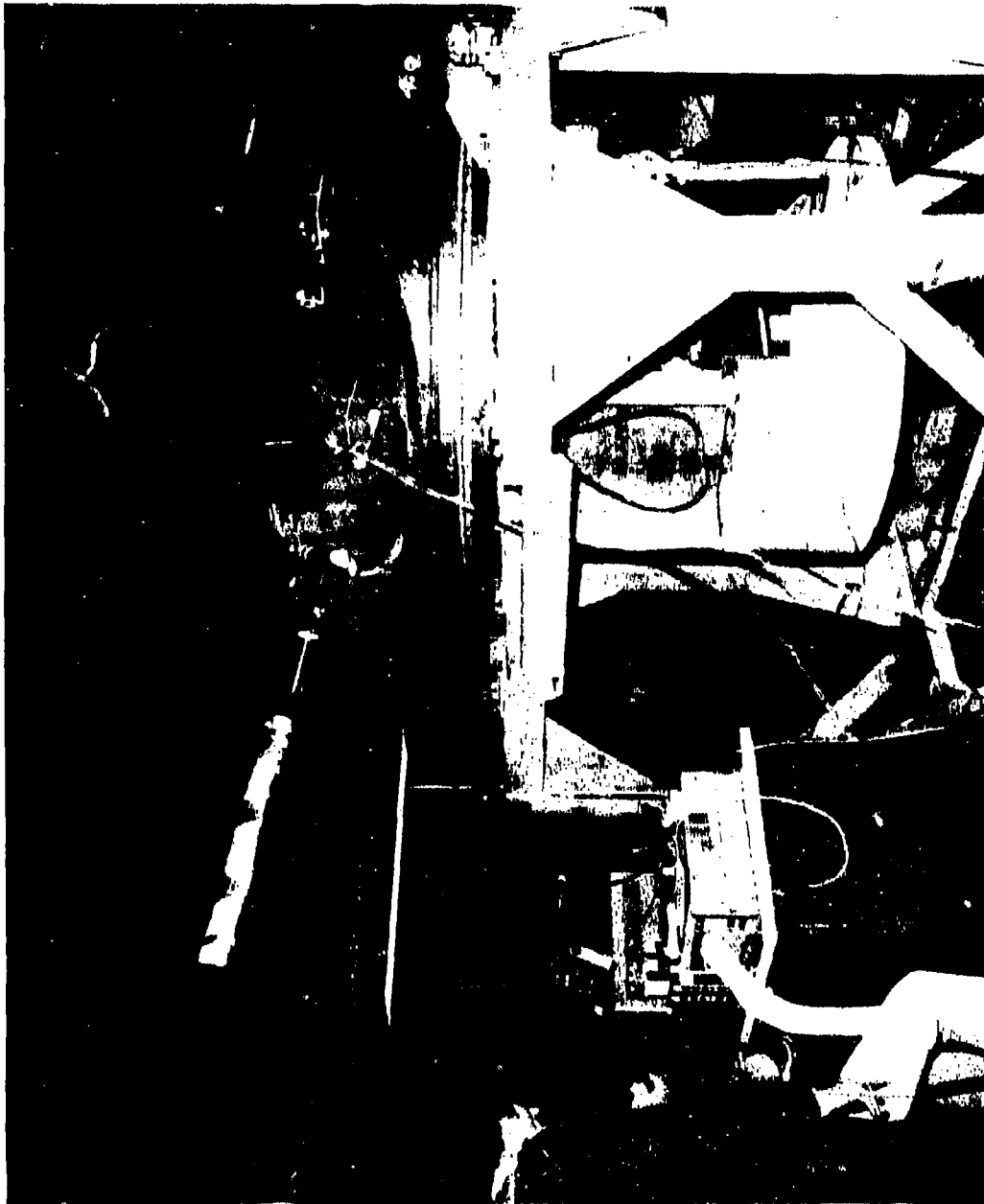
44

FIGURE 35

TURRET TEST FIXTURE

HEL FLUIDIC GUN STABILIZATION SYSTEM PROGRAM

45

MP-57251

CONTROLLER

FIGURE 36

TURRET TRUNNION AREA

SHOWING CONTROLLER INSTALLATION

HDL FLUIDIC GUN STABILIZATION SYSTEM PROGRAM

46

○   The desired disturbance suppression ratio of
20 decibels was not attained during the program.
This was attributed to the assumption of a plant
dynamic model which was inaccurate, resulting in
improper design of the dynamic characteristics
of the controller. Coulomb friction, of a
significant and unanticipated magnitude, was
present in the system. However, after the plant
dynamics were accurately determined, the
analytical model accurately predicted the
actual performance of the system.

5.2 Recommendations

On the basis of the foregoing, it is recommended that,
before designing a controller for a particular vehicle, an
accurate determination be made of the dynamic characteristics
of both the gun and the turret actuation system as well as the
characteristics of the vehicle suspension system. It is also
recommended that closed loop testing be included early in the
development program to uncover and correct any unanticipated
control system anomalies.

APPENDIX A

LINEARIZATION AND SIMPLIFICATION
OF A TANK GUN ACTUATION SYSTEM

APPENDIX A

LINEARIZATION AND SIMPLIFICATION
OF A TANK GUN ACTUATION SYSTEM

The pressure control servovalve is characterized by the following:

P_R command pressure differential, psid

P supply pressure = 1500 psi

P_L load differential pressure, psid

Q valve flow rate, cubic inches per second

K_Q droop constant, 20 psi per cubic inch per second

A_L area of pressure feedback land = 0.00985 square inch

A_R area of pressure command land = 0.0432 square inch

A_p piston area = 2.0 square inches

$\dot{y}$ piston velocity, inches per second

F force on spool, pounds

f friction constant on spool, $\dfrac{\text{lb-sec}}{\text{in.}}$

X spool displacement, inches

X_m maximum spool displacement, inches

Q_m maximum flow rate = 38.9 cubic inches per second

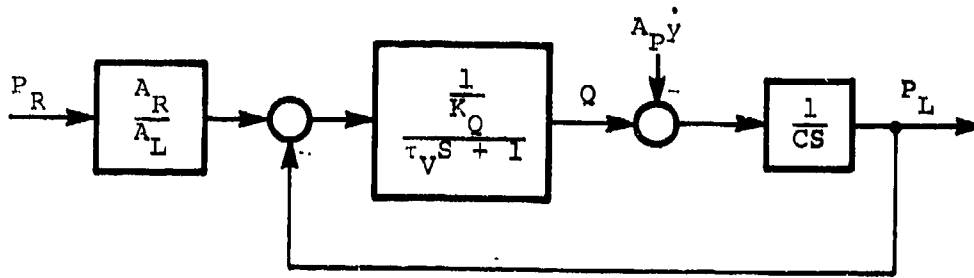C hydraulic capacitance, cubic inches per pound

A block diagram of the system is presented in the following sketch:
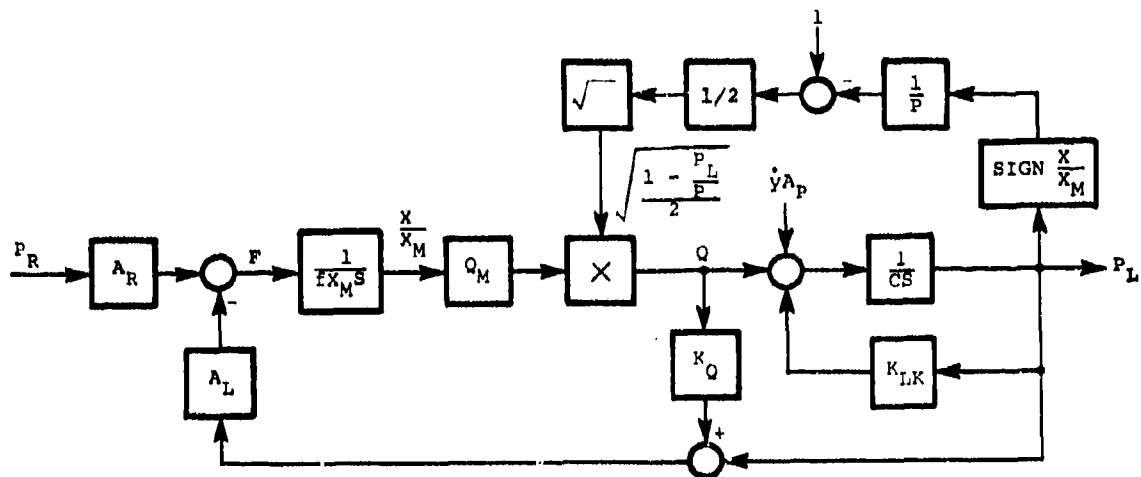
If it is assumed that only small perturbations of P_L about $P_L = 0$ are to be considered, and if leakage is neglected, then the block diagram can be reduced to:
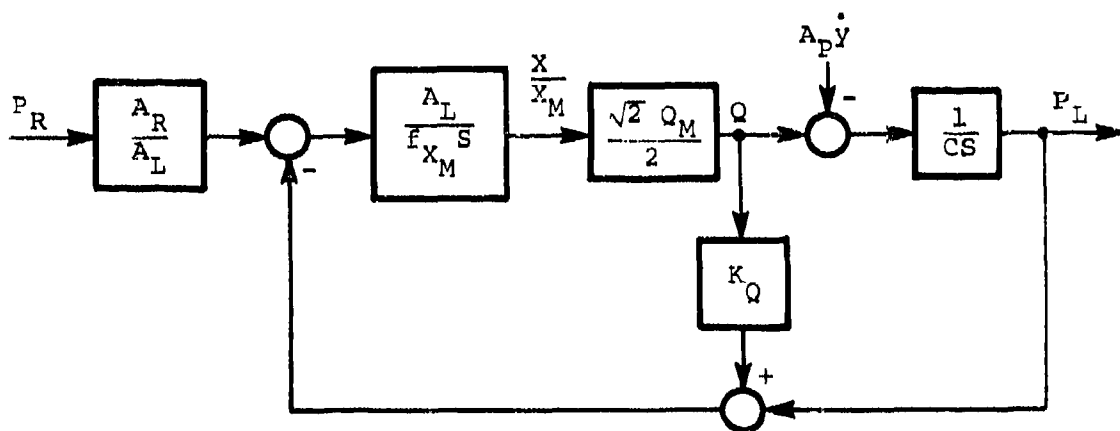
This further reduces to:

where $\tau_v = \dfrac{fX_m}{Q_m \, A_L \, K_Q \sqrt{2}}$.

The value given by MOOG for this time constant is $\tau_v = 0.016$ second.

Further reduction of the block diagram yields the following:
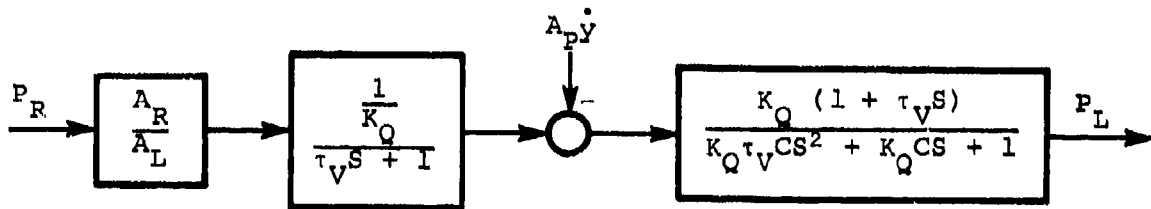
The capacitance associated with actuator volume in the MIC-V tank is given as,

$$C = 3.23 \times 10^{-5} \ \frac{\text{in.}^5}{\text{lb}}$$

Therefore,

$$\omega_n = \sqrt{\frac{1}{K_Q \tau_v C}} = 1080 \text{ radians per second;}$$

$$\zeta = 0.349 = \frac{1}{2} \sqrt{\frac{K_Q C}{\tau_v}}$$

If the approximation is made that

$$K_{\Omega}\tau_v CS^2 + K_Q CS + 1 \approx (\tau_v S + 1)(K_Q CS + 1),$$

the block diagram reduces to:
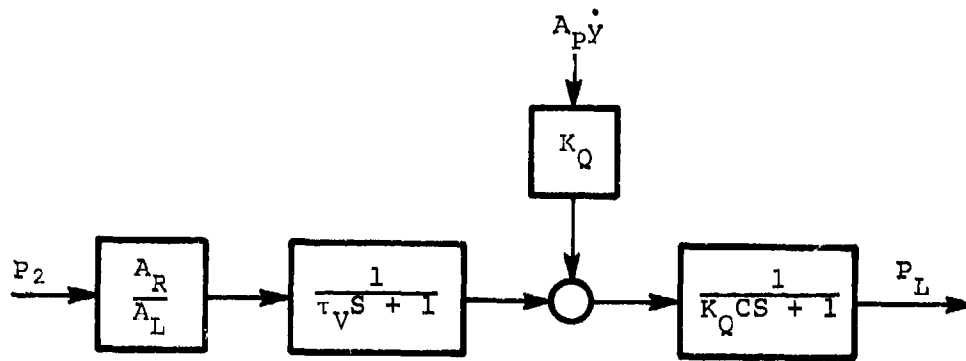
If further simplification is desired, the small time constants τ_v and $K_Q C$ may be ignored:

52

This simplified valve model is included in the following block diagram of the gun stabilization system.

G.D.   gun dynamics (bending)

A.D.   accelerometer dynamics

b_y actuator friction coefficient

β angle between actuator centerline and line connecting trunnion and actuator/gun attachment point

ℓ distance between trunnion and actuator/ gun attachment point

53

The servovalve/actuator/gun loop may be simplified as follows:

$$\begin{array}{ccc}
\boxed{K_Q A_P^2 + b_y} & \longleftarrow & \boxed{\ell \text{SIN}\beta} \longleftarrow \bigominus \longleftarrow \dot\theta_H \\
\end{array}$$

$$P_R \longrightarrow \boxed{\dfrac{A_P A_R}{A_L}} \longrightarrow \bigominus \longrightarrow \boxed{\dfrac{\ell \text{SIN}\beta}{I}} \longrightarrow \boxed{GD} \xrightarrow{\ddot\theta_G} \boxed{\dfrac{1}{S}} \xrightarrow{\dot\theta_G} \boxed{\dfrac{1}{S}} \xrightarrow{\theta_G}$$

$$P_R \longrightarrow \boxed{A_P A_R \over A_L} \longrightarrow \boxed{\dfrac{1}{\ell \text{SIN}\beta \,(K_Q A_P^2 + b_y)}} \longrightarrow \bigominus \longrightarrow \boxed{\dfrac{(\ell \text{SIN}\beta)^2 (K_Q A_P^2 + b_y)\,GD}{I}} \xrightarrow{\ddot\theta_G} \boxed{\dfrac{1}{S}} \xrightarrow{\dot\theta_G} \boxed{\dfrac{1}{S}} \xrightarrow{\theta_G}$$

with $\dot\theta_H$ entering the summing junction.

$$P_R \longrightarrow \boxed{\dfrac{A_P A_R}{A_L \,\ell \text{SIN}\beta \,(K_Q A_P^2 + b_y)}} \longrightarrow \bigominus \longrightarrow \boxed{\dfrac{S}{\dfrac{I S}{(\text{SIN})(K_Q A_P^2 + b_y)\,GD} + 1}} \xrightarrow{\dot\theta_G} \boxed{\dfrac{1}{S}} \xrightarrow{\theta_G}$$

with $\dot\theta_H$ entering the summing junction and $\ddot\theta_G$ output tap.

54
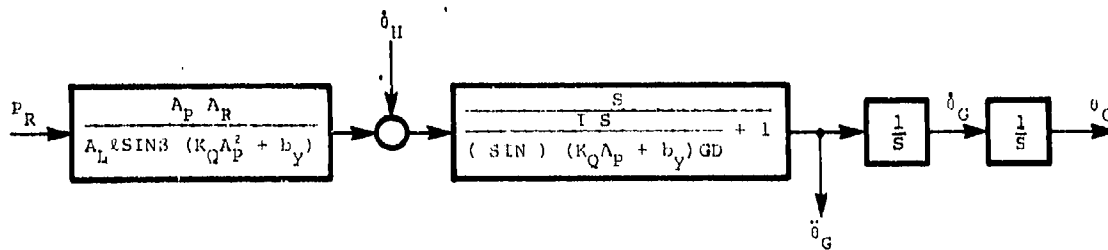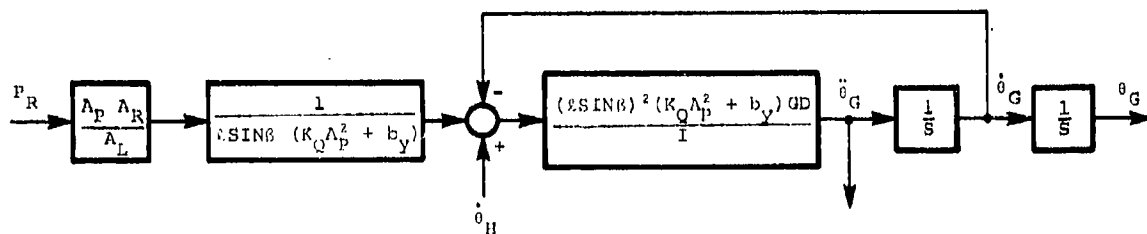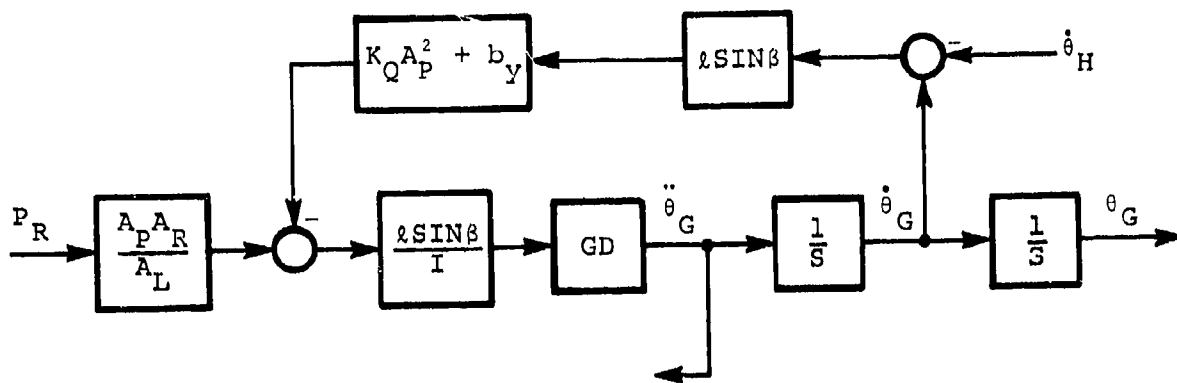
Ignoring gun bending: (GD = 1)
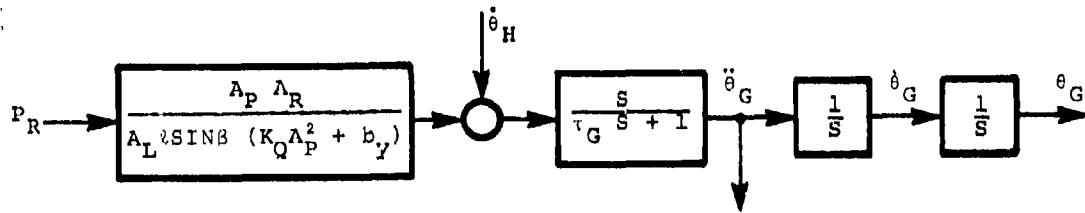
where $\tau_G = \dfrac{I}{(\ell \sin\beta)^2 (K_Q A_P{}^2 + b_y)}$

For MIC-V:

$$\tau_G = \frac{39.7 \quad (12)}{\left[8(0.82)\right]^2 \left[20(2)^2 + 0.15\right]} = 0.13 \text{ second}$$

For M60A1:

$$\tau_G = \frac{3813}{\left(12 \; 3.2(0.4)\right)^2 \left[11.11(4.72)^2 + 0\right]} = 0.78 \text{ second}$$

The gun stabilization system diagram with simplified pressure control servovalve, actuator and gun dynamics, and handle valve are shown below.
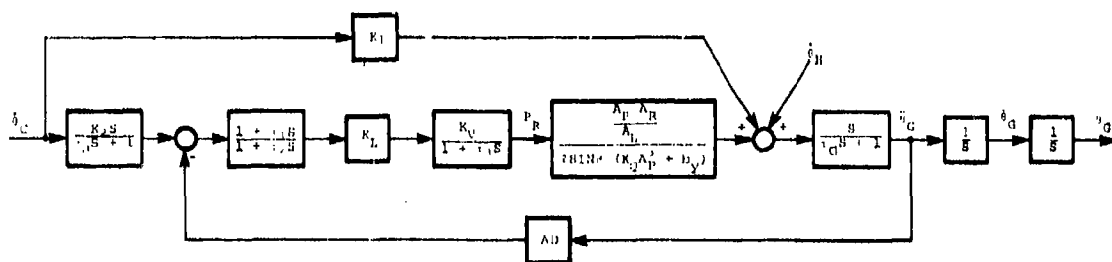
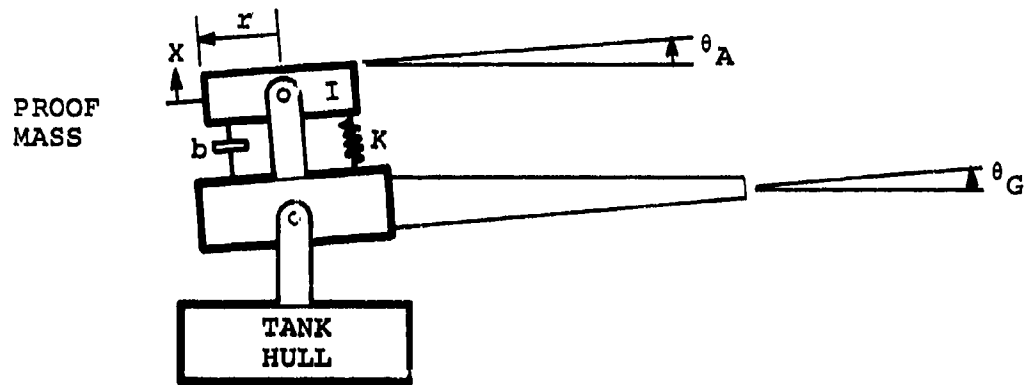Defining $K_v = \dfrac{A_L \ell \sin\beta (K_Q A_P{}^2 + b)}{A_P A_R}$
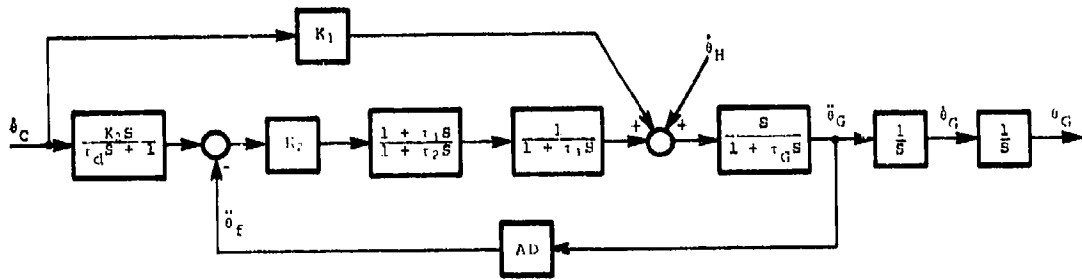
APPENDIX B

ACCELEROMETER TRANSFER FUNCTION,
GAIN, AND OPERATING RANGE

57

APPENDIX B

ACCELEROMETER TRANSFER FUNCTION, GAIN, AND OPERATING RANGE

Consider a proof mass accelerometer mounted on a gun, such that it senses angular motions of the gun about the elevation axis as shown in the following sketch:

where θ_A and θ_G are the angles of proof mass and gun centerlines with respect to the horizon, I is the angular moment of inertia of the proof mass, K is the angular spring constant, and b is the angular friction constant.

Motion of the proof mass is governed by the equation:

$$I\ddot{\theta}_A = -K(\theta_A - \theta_G) - b(\dot{\theta}_A - \dot{\theta}_G)$$

The following transfer function is then obtained:

$$\frac{\theta_A - \theta_G}{\ddot{\theta}_G} = -\frac{1}{S^2 + \frac{b}{I}S + \frac{K}{I}}$$

$$= -\frac{1/\omega_n^2}{\frac{S^2}{\omega_n^2} + \frac{2\zeta}{\omega_n}S + 1}$$

where

$$\omega_n^2 = \frac{K}{I}, \text{ and } \zeta = \frac{b}{2\sqrt{KI}}.$$

The relative angle, $\theta_A - \theta_G$, is determined by measuring the relative displacement X at the end of the proof mass so that

$$\frac{X}{\ddot{\theta}_G} = \frac{r}{\omega_n^2} \frac{1}{\frac{S^2}{\omega_n^2} + \frac{2\zeta}{\omega_n}S + 1}.$$

The steady-state sensitivity is:

$$\left.\frac{X}{\ddot{\theta}_G}\right|_{S \to 0} = \frac{r}{\omega_n^2}.$$

	DESIGNED C. Mafu	APPD	DATE
STARTED 5-21-76	APPD	DATE
FINISHED	APPD	DATE
REFERENCE		SCALE
WORK ORDER NO 3467- MODEL CYR713-CY-6100		

LAYOUT

FEATURED

NAME
FLUIDIC GUN
STABILIZATION
SYSTEM

CODE
AA 5

GARRETT MANUFACTURING DIVISION

DWG LAYOUT NO.
L 710538

SHEET

DISTRIBUTION LIST

Defense Documentation Center Cameron Station, Building 5 ATTN: DDC-TCA Alexandria, VA 22314	12 copies
Harry Diamond Laboratories ATTN: DRXDO-RCD (J. Goto) 2800 Powder Mill Road Adelphi, MD 20783	2 copies
Harry Diamond Laboratories ATTN: HDL Library 2800 Powder Mill Road Adelphi, MD 20783	3 copies
Harry Diamond Laboratories ATTN: Editorial Committee (Chairman) 2800 Powder Mill Road Adelphi, MD 20783	1 copy
Harry Diamond Laboratories ATTN: Branch 013 2800 Powder Mill Road Adelphi, MD 20783	1 copy
Harry Diamond Laboratories ATTN: Branch 014 2800 Powder Mill Road Adelphi, MD 20783	1 copy
U.S. Army Mobility Equipment Research and Development Command ATTN: DRXFB-EM (R. Ware) Fort Belvoir, VA 22060	5 copies
Naval Air Systems Command AIR 52022E (W. Langbrey) Washington, DC 20360	1 copy
Naval Ship Engineering Center Philadelphia Division ATTN: Code 6772 (D. Keyser) Philadelphia, PA 19112	1 copy
Naval Air Engineering Center (96213) Ground Support Equipment Department Lakehurst, NJ 08733	1 copy
U.S. Army TARADCOM ATTN: AMSTA-RKT (C. Bradley, Dr. R. Lee, and M. Steele) Warren, Michigan 48090	1 copy each